28th DeBeers Alex. Du Toit Memorial Lecture, 2004. On Cryogenian (Neoproterozoic) ice-sheet dynamics and the limitations of the glacial sedimentary record

Paul F. Hoffman
Department of Earth and Planetary Sciences
Harvard University, 20 Oxford Street, Cambridge, MA 02138, U.S.A.
e-mail: hoffman@eps.harvard.edu

ABSTRACT

The snowball earth hypothesis is a unified theory accounting for the global distribution of Cryogenian (roughly 720 to 635 Ma) glacial and glacial marine deposits, their global synchroneity demonstrated by chemostratigraphy, and their close association with thick carbonate strata and sedimentary iron deposits (banded iron formation) in certain areas. It postulates that on two separate occasions, around 710 and 640 Ma, the ocean froze over from pole to pole for long periods (*i.e.*, millions of years). The postulate has been widely criticized as being incompatible with the glacial sedimentary record indicating the former existence of fast-moving wet-base ice and open proglacial waters.

The younger Cryogenian glaciation in northern Namibia presents an excellent opportunity to investigate the sedimentary record. The area was then a vast shallow-water carbonate platform situated in the tropics or subtropics. The platform had a sharply-defined southern edge, beyond which a stratigraphically tapered foreslope wedge was descending into deep waters of the northern Damara extended terrain. The platform and foreslope were undergoing broad regional subsidence with no local structural deformation at the time of the younger glaciation. The Fransfontein Ridge (a present physiographic feature) is a simple homocline exposing a continuous 60-km-long section of the foreslope wedge. The western two-thirds of the ridge parallels the paleoslope contours 6 to10 km south of the foreslope-platform break, where the seafloor would have been 550 to 800 m below the top of the platform based on modern analogs. The eastern third of the ridge angles up the foreslope to the platform edge.

The Ghaub Formation is a sharply-bounded wedge of glacial marine strata that blankets the lower foreslope and tapers up-slope to a pinch-out 6±1 km south of the platform edge. It comprises a stack of marine till tongues (massive and poorly-stratified diamictites including debris flows, grounding-line proximal ‘rain-out’ and ice-contact diamictite) with subordinate stratified proglacial sediments variably rich in ice-rafted debris. The sediment is almost exclusively derived from the then top 60 m of the underlying carbonate (limestone and dolostone) platform and foreslope. Although most sediment transport indicators in the proglacial and subglacial strata are southerly-directed (*i.e.*, down-slope), rare starved ripple trains indicate traction currents flowing westward parallel to the paleoslope contours. These contour currents may imply open waters on the Damara seaway south of the platform.

The Ghaub Formation rests on a continuous erosion surface that carves out of the underlying strata a broad steep-walled trough, 0.1 km deep and ~18 km wide, assuming its axis is oriented roughly transverse to paleoslope contours. The glacial deposits average 80 m in thickness outside the trough, are attenuated on the sides of the trough, and form a steep moraine-like ridge in the trough axis. The ridge rises 600 m above the floor of the trough and is only 7.5 km wide at its base. It is composed of massive carbonate diamictite lacking proglacial strata. The ridge is interpreted as a transverse medial moraine formed near the mouth of a relatively narrow paleo-ice stream that eroded the trough. Ice streams are corridors of fast-flowing wet-base ice within an ice sheet and are thought to be responsible for up to 90% of the total ice drainage from the present Antarctic and Greenland ice sheets. Climate modeling suggests that annual mean surface temperatures on tropical continents with frozen oceans in the Cryogenian would have been similar to present Antarctica. Therefore, the existence of Cryogenian ice streams is not surprising and suggests that fast-flowing wet-base ice is not incompatible with a frozen ocean.

Directly below the trough is a 20 km-wide by 500 m-thick carbonate grainstone prism representing a complex of submarine channels and levees, showing that the area of the trough was a major submarine drainage system long before the glaciation began. It was localized by a tectonic subsidence anomaly going back to the time of the older glaciation, when the platform was undergoing active crustal stretching.

The moraine ridge was a prominent topographic feature at the end of the younger glaciation. The post-glacial cap dolostone was attenuated by winnowing on its flanks, but spectacular crystal fans of sea-floor aragonite (pseudomorphosed) are developed exclusively over the moraine in limestone directly above the cap dolostone.

The basal part of the Ghaub Formation outside the ice-stream trough contains a mappable ‘drift’ of terrigenous siltstone. The most likely source of this detritus is a regionally extensive sheet of fine-grained terrigenous sediment that is erosionally cut-out by the ice-stream trough. Accordingly, the entire Ghaub Formation outside and inside the trough must be younger than the cutting of the trough. If the trough was cut by an ice stream at a glacial maximum (or maxima), then the Ghaub Formation is entirely recessional. Sedimentary features (*e.g.*, ice-rafted debris, contour current indicators) within the Ghaub Formation do not represent conditions at the glacial maximum and do not constrain the extent of ocean ice cover at that time. If Cryogenian glacial deposits are recessional in other areas, issues still in dispute such as the maximum extent of marine ice cover will only be resolved with new geochemical data, for example iridium concentrations (cosmogenic dust proxy), boron isotopes (seawater pH proxy), and osmium isotopes (weathering proxy).

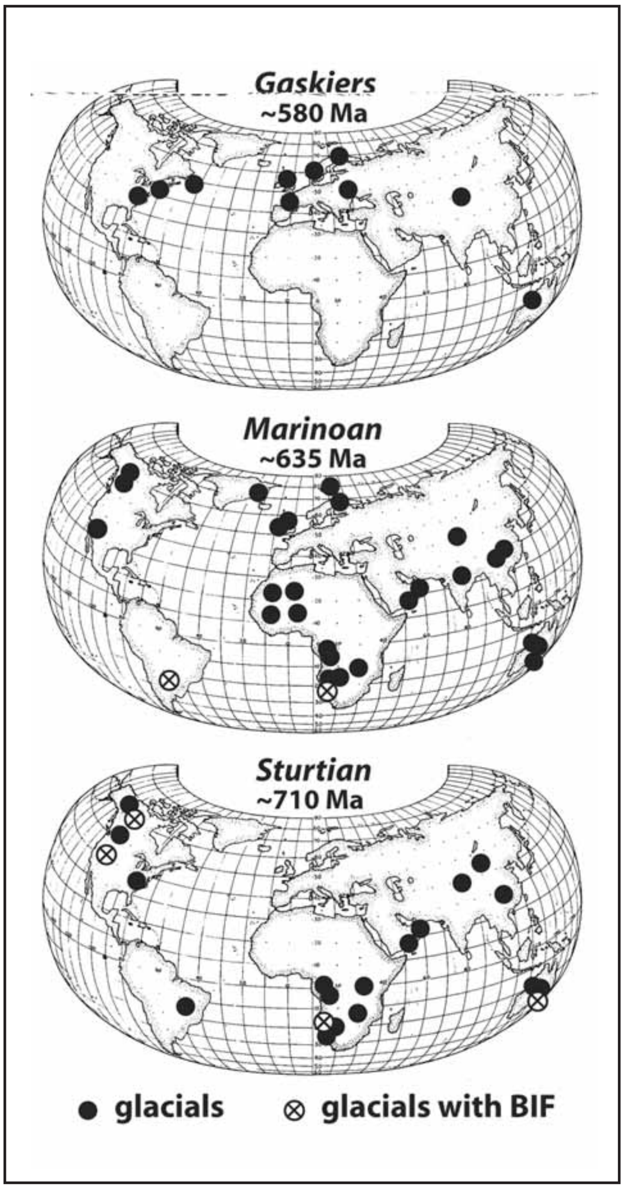

Figure 1. Global distribution of glacial or glacial marine strata ('glacials') of Ediacaran (*ca* 580 Ma), 'Marinoan' (*ca.* 635 Ma) and 'Sturtian' (*c.a.* 710 Ma) age (Table 1), showing occurrences of glacigenic banded iron formation (BIF). Raisz 'armadillo' projection.

Prologue

Reginald A. Daly (1871 to 1957) established the primacy of basalt in igneous petrogenesis and proposed the crustal assimilation theory of magma diversity. He was the only prominent North American (Canadian) geologist to actively support the continental displacement hypothesis of Alfred Wegener (1880 to 1930) and Alex Du Toit (1878 to 1949), popularly known as continental 'drift'. As the Sturgis Hooper Professor of Geology (1912 to 1942) at Harvard University, Daly lobbied the Carnegie Institution in Washington to sponsor Du Toit's 1923 investigation of South American geology bordering the South Atlantic, for the explicit purpose of testing the displacement hypothesis through comparative geology. The investigation provided indisputable proof that the displacement hypothesis was correct (Du Toit, 1927), although four decades elapsed before the proof was widely accepted. In *Our Mobile Earth*, published in 1926 at the height of the great debate over "drift", Daly argued that orogenic belts form where cold regions of the lithosphere founder and slide back into the mantle, causing adjacent buoyantly-stable regions to converge and collide. Daly developed a lifelong fascination with the geology of South Africa and his interpretation of the Vredefort ring-structure (Daly, 1947), published in his 76th year, is noteworthy not only for his advocacy of a planetoidal or asteroidal impact (then a radical idea), but also for his perception that the resultant crustal structure is largely due to "readjustments of the scarred and shattered terrain that were induced by the earth's gravitation". The paper is an excellent illustration of Daly's *credo* that field geology is the best teacher because it "exercises the imaginative muscle".

Introduction

Working backwards in time, the Cryogenian (Plumb, 1991) will be the next Period in Earth history to be defined stratigraphically after the Ediacaran. The end of the Cryogenian is placed at the termination of the Marinoan glaciation (Elatina Formation) in South Australia (Knoll *et al.*, 2004) and its beginning, yet to be formally defined, will be placed somewhere below the older Sturtian glacials or a correlative. The Cryogenian will be easy to remember as the time when the climate went crazy.

Two of the most severe glaciations in Earth history were the Sturtian around 710 Ma (Brasier *et al.*, 2000; Fanning and Link, 2004) and the Marinoan which ended in 635 Ma (Hoffmann *et al.*, 2004; Condon *et al.*, 2005). Glacial or glacial marine deposits from each event (Table 1) are globally widespread (Figure 1), and carbon-isotope seawater proxy data (Figure 2) imply that the glacial events were broadly synchronous (Knoll *et al.*, 1986; Kaufman *et al.*, 1997; Kennedy *et al.*, 1998; Walter *et al.*, 2000; Halverson *et al.*, 2005; Halverson, in press).

According to field-tested paleomagnetic data, Cryogenian continents were relatively dispersed and many impinged on or straddled the equator (Figure 3) (Embleton and Williams, 1986; Schmidt *et al.*, 1991; Kirschvink, 1992; Schmidt and Williams, 1995; Park, 1977; Sohl *et al.*, 1999; Evans, 2000; Kempf *et al.*, 2000; Evans *et al.*, 2001; Trindade *et al.*, 2003; Macouin *et al.*, 2004; Meert and Torsvik, 2004; Kilner *et al.*, 2005). Not since the Cambrian has a preponderance of continents been in the tropics. The situation should engender a cold global climate by increasing the rate of CO_2 consumption by silicate weathering (Marshall *et al.*, 1988; Worsley and Kidder, 1991; Donnadieu *et al.*, 2004a) and by raising the planetary albedo (Kirschvink, 1992).

In several regions, Cryogenian glacial deposits occur within thick, shallow-water, carbonate successions (Harland, 1965; Roberts, 1976; Gorin *et al.*, 1982; Narbonne and Aitken, 1995; Hoffmann and

Table 1. Correlation of Neoproterozoic glacials

Paleocontinent	Area	Sturtian	Marinoan	Ediacaran
Amazon	Alto Paraguay		Puga	
Angola	Nothern Namibia	Chuos	Ghaub	
Arabia	Mirbat	Lower Mirbat	unnamed	
	Oman Mtns	Gubrah	Fiq	
Australia	Adelaide	Pualco-Appila	Elatina	
	Central Australia	Areyonga	Olympic	
	Kimberleys	Walsh(?)	Landrigan	Egan
Avalon	Newfoundland			Gaskiers
Baltica	Oslo			Moelv
	Varanger Peninsula		Smalfjord	Mortensnes
Congo	West Congo	Lower Tilloid	Upper Tilloid	
	Zambia	Grand Congl.	Petit Congl.	
Kalahari	Gariep	Kaigas	Numees	
	Witvlei-Naukluft	Blaubekker	Blässkranz	
Laurentia	Alaska	Upper Tindir		
	British Columbia	Toby	Vreeland	
	Blue Ridge	Konnarock		
	California	Wildrose	Surprise	
	East Greenland	Ulvesø	Storeelv	
	East Svalbard	Petrovbreen	Wilsonbreen	
	Idaho	Scout Mountain		
	NW Territories	Rapitan	Stelfox	
	Scotland		Port Askaig	Loch na Cille
India	Lesser Himalaya		Blaini	
Mongolia	Central Mongolia	Tsagaan Oloom		
Sao Francisco			Macaubas	
South China	Guizhou	Chang'an	Nantuo	
Tarim	Quruqtagh	Bayisi(?)	Tereeken	Hankalchough
West Africa	Taoudeni		Jbéliat	
	Volta		Kodjari	

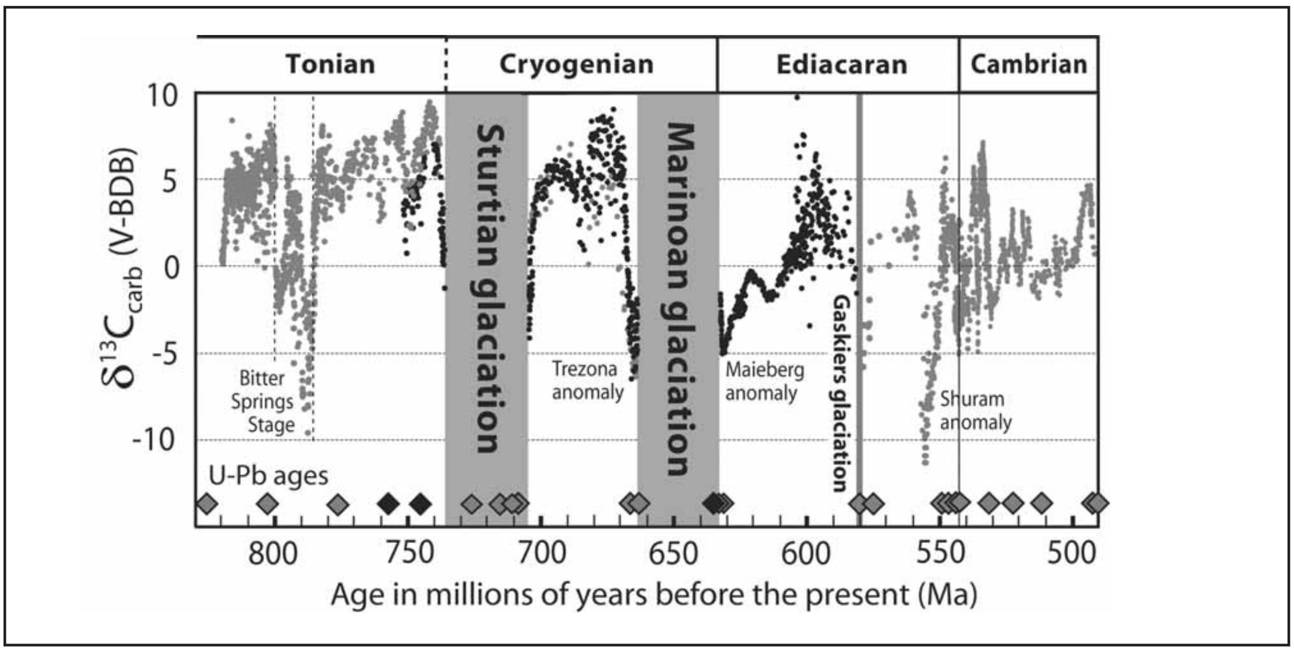

Figure 2. Provisional composite 820 to 490 Ma carbon isotopic record from marine carbonates in Australia, Canada, southern Namibia, Morocco, Oman, Svalbard and USA (grey dots) and the Otavi Group (black dots) in northern Namibia (see Halverson *et al.*, 2005; Halverson, in press, for data sources). Existing U-Pb zircon age control indicated by grey and black diamonds as above (see MacGabhann, 2005, for data sources). Note the long interval of generally elevated _^{13}C ~5‰ from 820 Ma until just before the Marinoan glaciation. Negative excursions of 10 to 15‰ frame the Sturtian and Marinoan glacials in different areas, proving the glaciations were globally synchronous.

Prave, 1996; Hoffman *et al.*, 1998; Halverson *et al.*, 2005). Non-skeletal carbonate (*e.g.*, Cryogenian) will always be preferentially produced in the warmest parts of the surface ocean because of its 'reverse' solubility (Broecker and Peng, 1982). Paleomagnetic data indicating low paleolatitudes for these successions (Trindade *et al.*, 2003; Macouin *et al.*, 2004; Kilner *et al.*, 2005; Maloof *et al.*, in press) demonstrate a normal

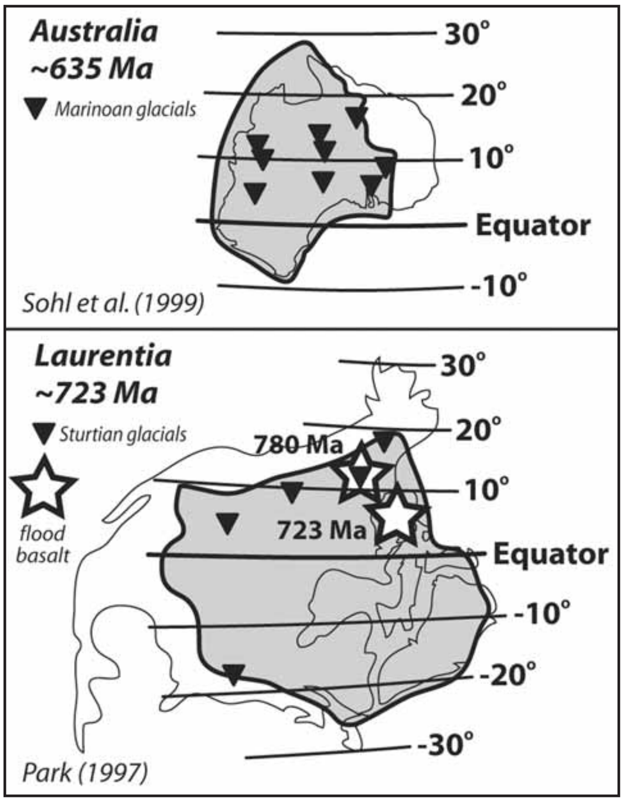

Figure 3. Paleomagnetically constrained paleogeography of Laurentia at 723 Ma (Park, 1997), showing distribution of Sturtian (*ca*. 710 Ma) glacials (Table 1), and of Australia during the Elatina (Table 1) glaciation (Sohl *et al.*, 1999), showing distribution of correlative Marinoan glacials. Eruption of Natkusiak flood basalt (723 Ma, Arctic Canada) close to the equator (star) must have caused atmospheric CO_2 to adjust lower for millions of years due to enhanced weathering.

meridional climate gradient (warmest at the equator) and the incursion of glaciers suggests that even the warmest areas were very cold.

Cryogenian glaciations were accompanied by major oceanic geochemical perturbations. Large-scale sedimentary hematite (Fe_2O_3) and manganese (MnO_2) deposits occur within glacial marine formations in Namibia (Martin, 1965), Australia (Whitten, 1970), Canada (Klein and Beukes, 1993) and Brazil (Klein and Ladeira, 2004). These non-volcanogenic banded iron (±manganese) formations (BIF) are unique in the last 1.89 Ga (Klein and Beukes, 1993; Klein and Ladeira, 2004). They indicate that the glacial deep waters went anoxic, allowing Fe^{2+} and Mn^{2+} ions supplied by mid-ocean ridge hydrothermal systems to travel widely in solution. Martin (1965) attributed the "peculiar combination of sediments" to "oxygen deficiency in stagnating bottom waters caused by an ice cover".

Conditions for BIF deposition are more stringent than Martin (1965) knew. Canfield and Raiswell (1999) pointed out that Fe^{2+} concentrations would remain low if the anoxic waters were euxinic (H_2S-rich), like the contemporary Black Sea, because the Fe would be titrated out in sedimentary sulfides. As H_2S is mainly the product of bacterial reduction of sulfate supplied by rivers, they postulated that a global glaciation would greatly lower the flux sulfate into the ocean, strangling the production of H_2S, and thereby allowing Fe^{2+} concentrations to rise. Bacterial sulfate reduction consumes organic matter, which would also be in short supply if the ocean was ice covered. Moreover, the reduction in water pressure on mid-ocean ridge hydrothermal systems accompanying a sea-level fall of >400 m, as would occur if the continents were mostly covered by ice sheets, would significantly increase the Fe/S vent flux ratio (Kump and Seyfried, 2005). The spotty distribution of glacigenic BIF (Figure 1) may reflect regional variability in Fe:S in an ocean that was poorly mixed because of an ice cover.

The dissolved Fe(II) must be oxidized to Fe(III) in order to precipitate as precursor to BIF. This could occur wherever oxic waters were supplied (*e.g.*, subglacial meltwater discharges at marine ice grounding lines) or by anoxygenic phototrophic bacteria (Kappler *et al.*, 2005) in marine areas where ice is cracked or thin.

More universal than BIF in their association with Cryogenian glacials are post-glacial 'cap' carbonates (Figure 4). These are continuous layers of dolostone, limestone, or rarely rhodochrosite ($MnCO_3$), that sharply blanket the glacial deposits without significant hiatus, or the sub-glacial erosion surface where glacials are absent (Aitken, 1991; Fairchild, 1993; Grotzinger and Knoll, 1995; Kennedy, 1996; Kennedy *et al.*, 1998, 2001; James *et al.*, 2000; Hoffman and Schrag, 2002; Nogueira *et al.*, 2003; Jiang *et al.*, 2004; Allen and Hoffman, 2005; Corsetti and Grotzinger, 2005; Shields, 2005). They were deposited on continental margins and inland seas globally, even in regions where carbonates are otherwise absent. The Marinoan (635 Ma) cap carbonate (Figure 4) is widely believed to have been deposited during the base-level rise attending rapid ice sheet recession, and it hosts a panoply of unusual sedimentary structures which occur in broadly the same stratigraphic sequence on many different continental margins (*e.g.*, Allen and Hoffman, 2005; Shields, 2005). Cap carbonates host a number of geochemical and isotopic anomalies, some of which bear on the extent and duration of ocean ice cover (*e.g.*, Bodiselitch *et al.*, 2005; Kasemann *et al.*, 2005).

Carbonate and silicate weathering of globally glaciated landscapes under high CO_2 radiative forcing can quantitatively supply the alkalinity needed for cap carbonates (Higgins and Schrag, 2003). In addition, 1 to 2 m of carbonate could result from glacio-eustatic changes (the 'coral reef' hypothesis of Berger, 1982) in the absence of calcifying organisms (Ridgwell *et al.*, 2003; Ridgwell and Kennedy, 2004). A similar quantity is hypothesized to have resulted from anaerobic oxidation of methane released from tropical shelf permafrost and submarine gas hydrates (Kennedy *et al.*, 2001; Jiang *et al.*, 2003). This process depends on sulfate to be the electron acceptor (Boetius *et al.*, 2000) because aerobic methane oxidation (by O_2) does not produce alkalinity.

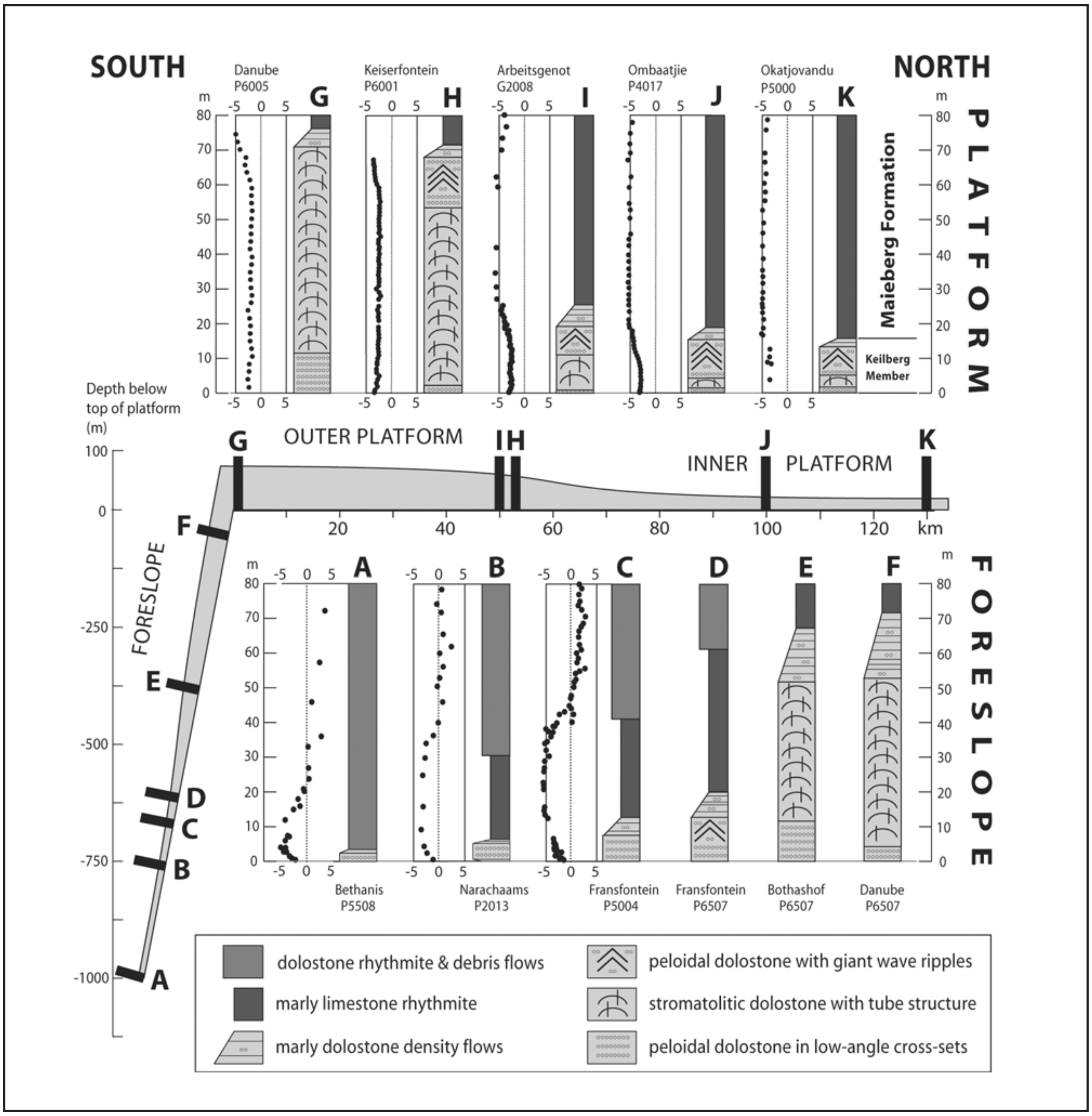

Figure 4. Variation in thickness and lithofacies of the 635 Ma post-glacial cap dolostone (Keilberg Member) across the Otavi Group platform and foreslope (Figure 7, 8) in northern Namibia (Hoffman and Halverson, in press). Cap dolostone rests sharply on glacial marine strata (Ghaub Formation) on the lower foreslope, on pre-glacial carbonates (Ombaatjie Formation) on the upper foreslope and outer platform, and on a discontinuous veneer of diamictite on the inner platform. Average thickness of the transgressive cap dolostone (*sensu stricto*) is ~30 m.

What is the snowball earth hypothesis?

In a nutshell, the snowball earth hypothesis (Kirschvink, 1992; Caldeira and Kasting, 1992) postulates that the ocean froze over from pole to pole for long periods during the Sturtian and Marinoan glaciations. It attempts to explain all the observations outlined above in a unified theory (Hoffman and Schrag, 2002).

The hypothesis invokes a fundamental instability, or 'bifurcation', in the climate system due to ice-albedo feedback: if the global area of ice and snow exceeds a critical value, the cooling caused solely by the increased reflection of incoming solar radiation becomes self-sustaining and quickly drives ice lines to the equator (Figure 5). The instability is a robust feature of simple energy-balance climate models (Budyko, 1969; Sellers, 1969; Lindzen and Farrell, 1977; North *et al.*, 1981; Caldeira and Kasting, 1992) and many coupled atmospheric general circulation models (Jenkins and Smith, 1999; Hyde *et al.*, 2000; Baum and Crowley, 2001; 2003; Donnadieu *et al.*, 2003; Lewis *et al.*, 2003; Peltier *et al.*, 2004; Pollard and Kasting, 2004). Adjusted for Cryogenian ambience (*e.g.*, reduced Solar luminosity, faster Earth rotation rate, *etc.*), most simulations find the critical point in CO_2 radiative forcing at 1-2 PAL (present

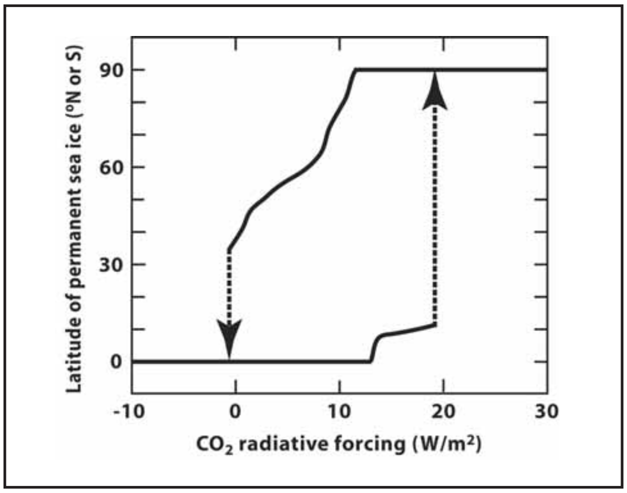

Figure 5. Latitude of the perennial ice edge versus CO_2 radiative forcing in a seasonal energy-balance climate model with fully-coupled sea-glacier dynamics, applied to a zonally symmetric all-ocean planet (Pollard and Kasting, 2005). The CO_2 radiative forcing is applied as a uniform decrement to the outgoing planedtary infrared radiation, representing variations in atmospheric CO_2 amount relative to today (Hyde *et al.,* 2000; Crowley *et al.,* 2001). Ice with low bubble density is prescribed in the model run, yielding thin ice (<2 m) at latitudes <10º (Pollard and Kasting, 2005)

atmospheric level). The corresponding ice-line latitude is ~35º (Pollard and Kasting, 2005).

With the ocean frozen over, surface temperatures fall below freezing everywhere. Silicate weathering (a sink for CO_2) is greatly diminished and consequently the CO_2 emitted from subaerial and submarine volcanic vents slowly builds up in the atmosphere and ocean. The CO_2 radiative forcing required to melt the snowball earth is uncertain (Pierrehumbert, 2004; 2005; Pollard and Kasting, 2005), but achieving it could take millions or even tens of millions of years of normal volcanic outgassing, depending on the type of snowball earth (see below). On this time scale, CO_2 exchange through sea-ice cracks and leads will keep the atmosphere and ocean in equilibrium, but O_2 invasion will be unable to overcome the sinks for O_2 within the ocean (Jeff Severinghaus, personal communication). When the CO_2 radiative forcing finally overcomes the snowball albedo, meltdown should occur rapidly (*e.g.,* ~2 kyr, Hyde *et al.,* 2000) due to reverse ice-albedo and other feedbacks. Meltwater production rates could approach 10 Sv [1.0 Sv (Sverdrup) = 10^6 m^3 s^{-1}, or roughly the mean global runoff rate] causing ocean hyperstratification (Hoffman, 1999; Hoffman *et al.,* 2004; Shields, 2005). Because the time-scale for CO_2 drawdown by silicate weathering is 1 to 3 orders of magnitude longer than the estimated deglaciation time, the meltdown will be followed by a greenhouse transient, the signature of which is the post-glacial cap carbonate (Hoffman *et al.,* 1998; Higgins and Schrag, 2003), which has no quantitative Phanerozoic counterpart.

Sea-glacier dynamics on snowball earth

On a snowball earth, the steady-state thickness of stationary floating ice varies inversely with surface air temperature, being thicker at the poles and thinner at the equator. This is because the geothermal heat supplied to the base of floating ice is nearly the same everywhere. Extratropical ice is sufficiently thick (~1.0 km) that it flows under its own weight in the direction of taper. In dynamic steady state, the flowage of ice is balanced by sublimation and basal melting in the tropics, and by condensation (snowfall) and basal freezing in the extratropics. Maximum flow velocities are in the same range as mountain glaciers, 10s to 100s m yr^{-1} (Goodman and Pierrehumbert, 2003; Pollard and Kasting, 2005). Warren *et al.* (2002) call this 'sea glacier' ice as it can include 'sea ice' (*i.e.,* frozen sea water) and ice-shelf ice (*i.e.,* compacted snow, mostly glacier ice that has flowed across a grounding line). Multi-year sea ice is brine-free and has a signficantly lower albedo than ice formed by compaction of snow, which is full of bubbles (Warren *et al.,* 2002). Tropical ice albedo has a critical bearing on the thickness of the tropical sea glacier (Pollard and Kasting, 2005), the radiative forcing required for deglaciation (Pierrehumbert, 2004; 2005), and consequently on the duration of a snowball earth.

Three solutions for Cryogenian glaciation (Figure 6) have emerged from numerical simulations incorporating sea-glacier dynamics (Goodman and Pierrehumbert, 2003; Peltier *et al.,* 2004; Pollard and Kasting, 2005). Each has different implications for the duration of the glaciation, the nature of the glacial termination, and the stress imposed on the biosphere both during and after glaciation (Pollard and Kasting, 2005). The first solution is characterized by thick (>100 m) tropical sea glaciers maintained by flowage from higher latitudes (Warren *et al.,* 2002; Goodman and Pierrehumbert, 2003). This 'thick ice' solution presents the greatest challenge to phototrophs and their dependents – where liquid water exists there is no light, where light exists there is no liquid water – although flowage-induced crack systems would offer extensive refugia wherever the sea glaciers touch bottom or landfast ice (Gaidos *et al.,* 1999). Juvenile sea ice formed in cracks contains brine channels that host a diverse microbiota (Thomas and Dieckmann, 2002). The biota must be tolerant of hyperoxia because photosynthetic O_2 is trapped in the brine channels. This might be an interesting pre-adaptation (Adam Maloof, personal communication) if atmospheric O_2 levels rose in the early Ediacaran (Canfield and Teske, 1996). The CO_2 radiative forcing required to terminate a 'thick-ice' snowball is possibly prohibitive (>550 PAL, Pierrehumbert, 2004; 2005).

A less daunting solution has recently been proposed (Pollard and Kasting, 2005), wherein the limit of km-thick ice is closely tied to the snow line. This model features narrow transition zones, between ~13º and 10º latitude, while the equatorial ocean is covered by broken sea ice <2 m thick, which is compatible with "healthy rates" of photosynthesis (Pollard and Kasting,

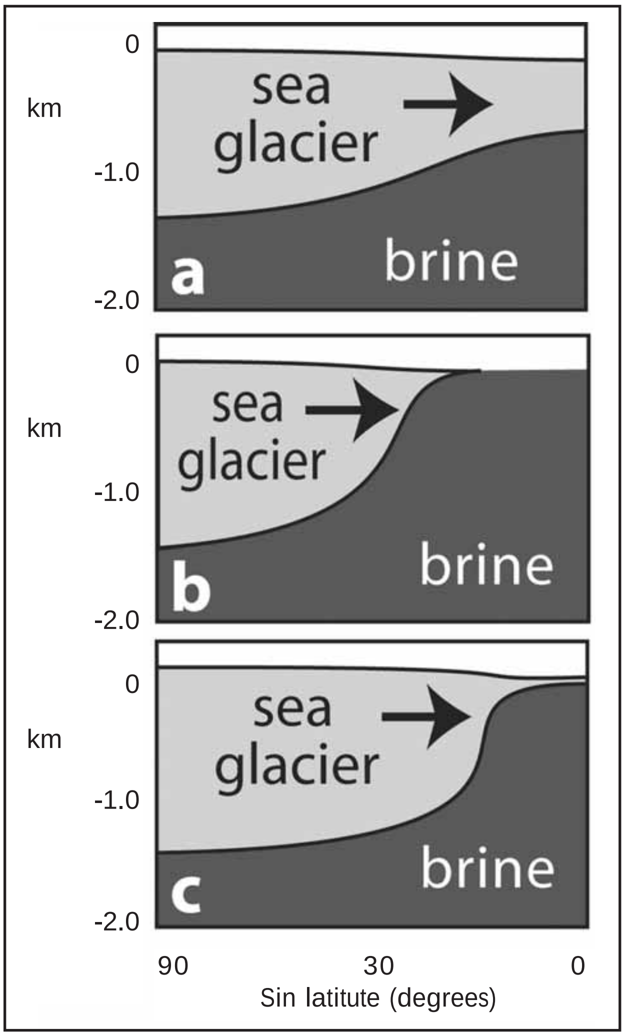

Figure 6. Three model scenarios of sea-glacier dynamics on planets with CO_2 radiative forcing set sufficiently low that ice sheets form on low-latitude continents (not shown): (**a**) thick tropical ice model (Goodman and Pierrehumbert, 2003; Warren *et al.*, 2002), (**b**) tropical oasis (aka 'slushball') model (Peltier *et al.*, 2004; Hyde *et al.*, 2000), and (**c**) thin tropical ice model (Pollard and Kasting, 2005; McKay, 2000).

2005). The broadband albedo of clear thin ice is ~0.45, significantly more absorbtive than the thick ice albedo of ~0.64 (Pollard and Kasting, 2005). Therefore, the glacial duration and the terminal 32 PAL of CO_2 are correspondingly lower than for the thick ice solution. The thin-ice solution is highly sensitive to equatorial ice albedo: it requires clear ice (basal freeze-on) to the exclusion of bubbly glacial ice (Pollard and Kasting, 2005). Impurities can lower (dust) or raise (salt) the ice albedo (Warren *et al.*, 2002).

The most lenient solution is the 'tropical oasis' model (Hyde *et al.*, 2000; Peltier *et al.*, 2004), in which an ice-covered supercontinent extends from pole to equator while almost half the total area of the ocean remains ice free. Interestingly, isolated marine platforms situated on the equator close to the supercontinent develop independent ice sheets, presumably due to the lowering of base level by 400 m in the model in response to the growth of the supercontinental ice sheet (Peltier *et al.*, 2004). It is not known if the ocean would become anoxic in this model, although the Fe: S ratio should rise with limited runoff (Canfield and Raiswell, 1999) and lowered sea-level (Kump and Seyfried, 2005). As the terminal radiative forcing is relatively low in the oasis model (Peltier *et al.*, 2004), it is perhaps the least satisfactory as an explanation for the Marinoan cap carbonate (Pollard and Kasting, 2005). The paleogeography used in the oasis model (Hyde *et al.*, 2000; Peltier *et al.*, 2004) favours ice-sheet flowage to the equator but it is inappropriate for the Cryogenian. It is inconsistent with paleomagnetic evidence for low-latitude Cryogenian continents and would in fact produce a relatively warm global climate if CO_2 levels were not prescribed but allowed to self-adjust through silicate weathering feedback (Marshall *et al.*, 1988; Worsley and Kidder, 1991; Schrag *et al.*, 2002; Donnadieu *et al.*, 2004b).

It is clear from the contrasting results of the modeling experiments and their sensitivity to input parameters that, for the time being at least, the geological record must serve as the court of last appeal regarding the extent and duration of ice cover on the ocean. The prime witnesses are expected to be geochemical and geochronological (*e.g.*, Bodiseltich *et al.*, 2005; Kasemann *et al.*, 2005).

Grounded ice-sheet dynamics

The dynamics of Cryogenian ice sheets (*i.e.*, large masses of grounded ice that flow from central regions of accumulation toward peripheral zones of ablation) is imprinted on the physical stratigraphic record of erosion and sedimentation (*e.g.*, Spencer, 1971; Edwards, 1984; Deynoux, 1985; Hambrey and Spencer, 1987; Preiss, 1987; Brookfield, 1994; McMechan, 2000; Kellerhals and Matter, 2003; Allen *et al.*, 2004). Virtually all students of Cryogenian glacial and glacial marine sediments have been impressed by their lithological similarity to Quaternary and Recent deposits. For some, this implies that the Cryogenian glaciations were regional in extent and globally diachronous (Crowell, 1983; 1999; Eyles, 1994; Young, 1995; Eyles and Januszczak, 2004). This view casts aside the chemostratigraphic evidence for synchroneity (Knoll *et al.*, 1986; Kaufman *et al.*, 1987; Kennedy *et al.*, 1998; Halverson *et al.*, 2005) and the arguments for low-latitude glaciation from paleomagnetism the carbonate-glacial association (Harland, 1965; Roberts, 1976; Schmidt and Williams, 1995; Evans, 2000; Hoffman and Schrag, 2002). Others accept these arguments but infer from the sedimentary record that the tropical ocean was never ice covered. The inferences are both direct and indirect. Open water is inferred indirectly from the thickness and character of Cryogenian diamictites and associated facies, which imply dynamic, wet-base ice, assumed to be incompatible with the cold and dry climate of a snowball earth (*e.g.*, McMechan, 2000a; b; Leather *et al.*, 2002; Kellerhals and Matter, 2003).

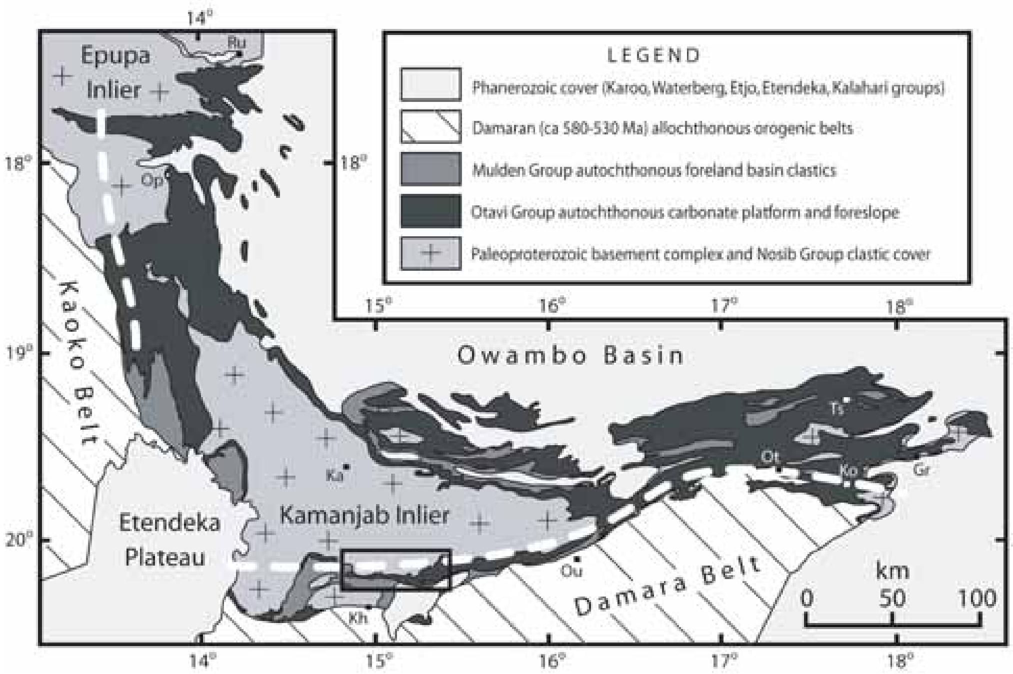

Figure 7. Outcrop belt of the autochthonous Otavi Group in northern Namibia (Hedberg, 1981), showing approximate trace of the foreslope-platform break (dashed white line). Rectangular box gives location of the Fransfontein Ridge. Towns: Gr, Grootberg; Ka, Kamanjab; Kh, Khorixas; Ko, Kombat; Op, Opuwa; Ot, Otavi; Ou, Outjo; Ru, Ruacana; Ts, Tsumeb.

The last link in that chain of logic was challenged by Donnadieu *et al.* (2003), who carried out numerical simulations of the growth and dynamics of continental ice sheets both before and after a tropical ocean freeze-over (see also Pollard and Kasting, 2004). Within 400 kyr of the snowball onset, low latitude continents in their model are largely covered by 2 to 4 km of ice. The accumulation zones of these ice sheets are warm base and the peripheral ablation zones are mainly cold base, but with narrow transverse corridors of fast-flowing, wet-base ice (Donnadieu *et al.*, 2003). Analogous ‘ice streams’ account for up to 90% of all the ice discharged from the present Antarctic and Greenland ice sheets (Bentley, 1987; Bamber *et al.*, 2000; Bennett, 2003), and transverse troughs 10s-100s km wide on the West Antarctic and Polar North Atlantic continental shelves were eroded by ice sheets during Quaternary ice maxima (Ó Cofaigh *et al.*, 2002; Heroy and Anderson, 2005; Ottesen *et al.*, 2005; Stoker and Bradwell, 2005). Large morainal buildups around the mouths of these paleo-ice streams (Ó Cofaigh *et al.*, 2003; Ottesen *et al.*, 2005; Stoker and Bradwell, 2005; McMullen *et al.*, in press) demonstrate the sediment-transport potency of the ice streams. As surface temperatures on tropical continents would be similar to those on contemporary Antarctica if the tropical ocean were frozen, the existence of dynamic, wet-base ice should not rule out a frozen ocean (Donnadieu *et al.*, 2003). The common tendency for Cryogenian glacial deposits (Hambrey and Harland, 1981) to be locally thick (100s to 1000s of meters) but regionally thin (10s of meters) provides some support for Donnadieu *et al.* (2003), but no Cryogenian ice stream has previously been recognized.

There is direct evidence for open water within Cryogenian glacial marine sequences, but the glacial stage they represent is generally uncertain. The evidence includes stratified proglacial sediments with far-travelled ice-rafted debris (IRD), including iceberg ‘dumps’ (Condon *et al.*, 2002). This implies an iceberg calving line close to the ice grounding line because icebergs calved from broad ice shelves are generally free of debris (Carey and Ahmad, 1961; Drewry and Cooper, 1981; Orheim and Elverhoi, 1981; Alley et al., 1989). The inference (Condon *et al.*, 2002) hinges on the identification of iceberg ‘dumps’, without which the IRD could have been released close the grounding line from ice-shelf ice of unlimited extent. Evidence of a different type includes starved ripples in stratified proglacial sediments produced by bottom traction currents flowing parallel to paleoslope contours (described below). Such gyre-like currents imply wind-driven circulation of adjacent basin surface waters. Microfossils or molecular fossils (biomarkers) in glacial marine strata that are diagnostic of phototrophy are said to rule out a snowball earth of the thick-ice type (Corsetti *et al.*, 2003; Olcott *et al.*, 2005) but only if productivity in crack systems is neglected. All these lines of evidence share a common limitation, which is the degree to which the existing sedimentary record represents the complete glacial cycle, the ice maximum most importantly. The data to be presented bear on this issue.

In order to shed light on Cryogenian ice-sheet dynamics, the younger glaciation ending in 635 Ma (Hoffmann *et al.*, 2004; Condon *et al.*, 2005) was targeted for study in northern Namibia. The paleo-environmental range of the host succession allows patterns of glacial erosion and deposition to be worked out on the regional scale (Halverson *et al.*, 2002). The host succession is carbonate-dominated, allowing its physical and isotopic stratigraphies to be mapped out in detail (Halverson *et al.*, 2005; Hoffman and Halverson, in press). The glaciation occurred on a simple flat-topped marine platform undergoing broad regional subsidence without local structural complication. The exposure in the area is exceptional, given 200-600 m of local topographic relief and sparse vegetation (precipitation rates <25 cm yr^{-1}). Moreover, the carbonate-glacial association so well displayed in Namibia lies at the core of the Cryogenian climatic paradox. What follows is a preliminary report on a continuous 60 km-long section of the southern foreslope exposed on the Fransfontein (Franni-aus) Ridge (Figure 7).

Otavi Group carbonate platform and foreslope

From late Tonian through early Ediacaran time (roughly 770 to 590 Ma), a vast (>10^5 km^2), 3 to 4 km-thick, shallow-water, carbonate platform (Figure 8) developed across northern Namibia (Halverson *et al.*, 2005; Hoffman and Halverson, in press). The southern edge of the platform (Figure 7) is sharply defined by primary facies changes and is bordered by a stratigraphically tapered foreslope wedge. The platform and its foreslope developed in two stages: a rift stage dominated by active, south-dipping, crustal-scale, normal faults with back-rotated (northward-tilted) footwalls, and a sag stage with broad regional subsidence and modest foreslope progradation.

Two discrete glacigenic formations divide the carbonate-dominated succession into three subgroups (Hoffmann and Prave, 1996). The older one (Chuos Formation) has been correlated with the global 'Sturtian' glaciation (Kennedy *et al.*, 1998) and it unconformably overlies volcanics dated at 746±2 Ma (Hoffman *et al.*, 1996). This glaciation occurred during the rift stage of

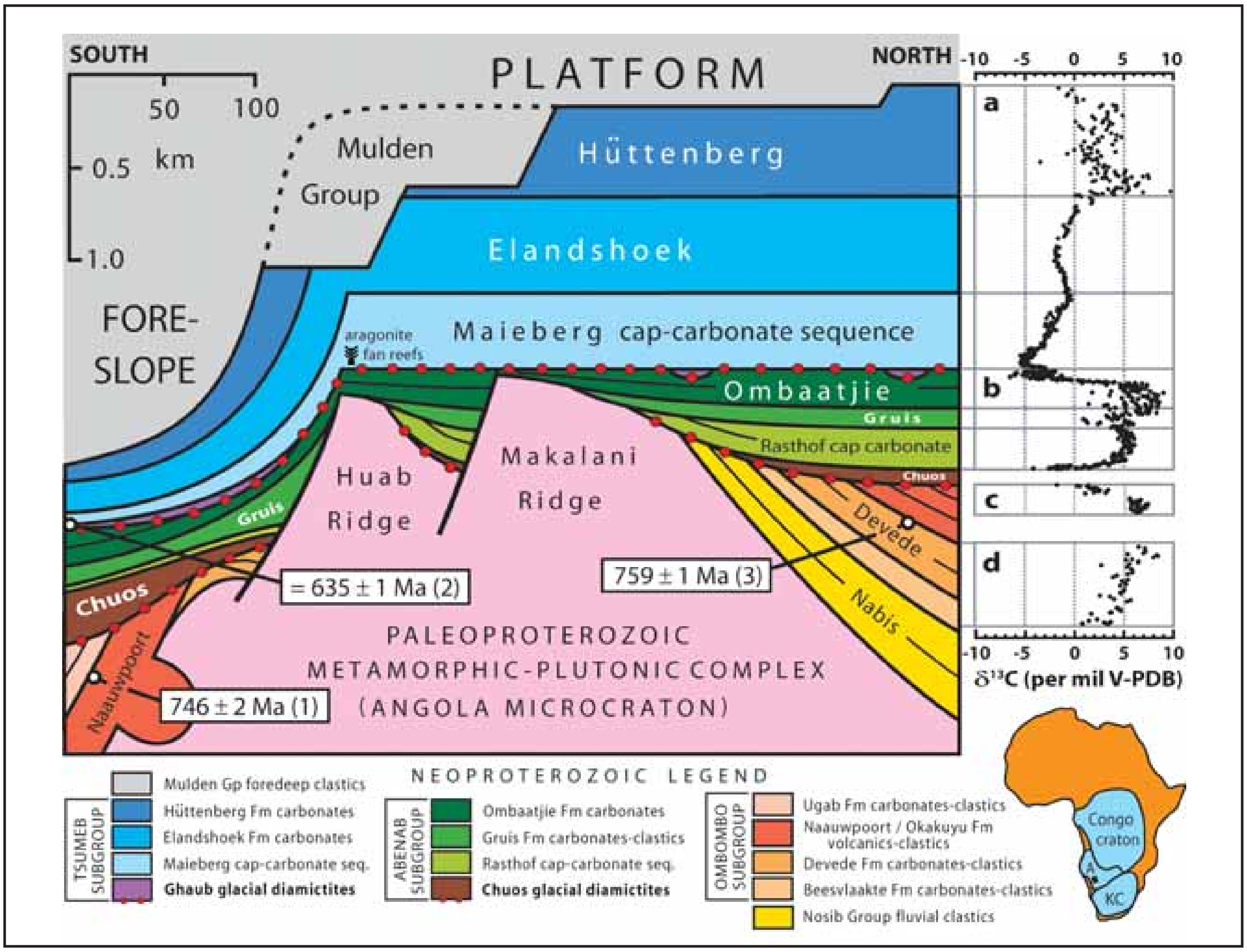

Figure 8. Generalized north-south stratigraphic cross-section of the Otavi Group in the western half of the outcrop belt (Figure 7). Representative carbon isotope profiles for the Tsumeb (**a**), Abenab (**b**), Ugab (**c**), and Ombombo (**d**) subgroups from Hoffman and Halverson (in press). U-Pb zircon ages from (1) Hoffman *et al.* (1996), (2) Hoffmann *et al.* (2004), and (3) Halverson *et al.* (2005). Inset map: A, Angola microcraton; KC, Kalahari craton.

the Otavi Group. The younger one (Ghaub Formation) has been correlated with the global 'Marinoan' glaciation (Kennedy *et al.,* 1998) and its basinal equivalent contains a volcanic ash dated at 635.6±0.6 Ma (Hoffmann *et al.*, 2004). This glaciation occurred during the sag stage and it is the focus of this report.

The distribution and thickness of the Ghaub Formation are controlled by the platform-foreslope paleotopography. A patchy veneer of carbonate diamictite (rarely >2.0 m thick) extends for 300 km across the platform to within 60 km of the southern edge. The diamictite is virtually non-existent on the outer platform and upper foreslope, within 60 and 6 km, respectively, of the southern edge. The diamictite lies upon a continuous erosion surface that is structurally paraconformable on the regional scale (Halverson *et al.*, 2002). The surface has <60 m of local relief with respect to the underlying parasequences of the Ombaatjie Formation and a zone of maximum erosion occurs 90 to 130 km from the edge (Halverson *et al.*, 2002). A lithologically distinctive, post-glacial, 'cap' dolostone (*sensu* Kennedy, 1996) overlies the diamictite sharply but without significant hiatus or reworking. It lies directly on (and identifies) the sub-glacial erosion surface wherever the diamictite is absent. The cap dolostone is a uniform 10-20 m in thickness over most of the platform but swells to 50 to 75 m thick within 75 km of the southern edge (Figure 4). These field relationships have been tested by _^{13}C profiling in >30 measured sections (Halverson *et al.*, 2002; Hoffman and Halverson, in press).

A continuous wedge of Ghaub Formation drapes the lower foreslope. Its zero isopach lies 6±1 km seaward of the foreslope-platform break, which (for comparison) corresponds to water depths of 600 to 650 m on the prograded western slope of the modern Great Bahama Bank. The wedge is dominantly composed of non-stratified, marine ice grounding-line diamictites and derived gravity flows. A subordinate component consists of stratified, proglacial deposits (plume fallout, sediment density flows, and rare contourites) that are generally rich in ice-rafted debris (IRD). The glacially-transported debris is almost entirely derived from four sources: platformal marine parasequences b7 and b8, a subsequent carbonate aeolianite (b9) relicts of which occur at the southern edge, and a broadly contemporaneous low-stand wedge (Franni-aus Member) occurring directly beneath the Ghaub Formation on the lower foreslope. We interpret the aeolianite and low-stand wedge as expressions of falling base level associated with ice-sheet growth at higher latitudes.

Foreslope sedimentation before the Ghaub glaciation

The longest continuous exposure of the Otavi foreslope is on the Fransfontein Ridge (FR), a structurally simple, south- and southeast-dipping homocline (Figure 9). The western two-thirds (40 km) of the ridge (sections 1 to 25) roughly parallels the inferred foreslope countours and lies 5 to 10 km seaward of the projected southern edge (equivalent to water depths of 550 to 800 m off the Great Bahama Bank). The eastern third (sections 25 to 32) bends to the northeast and climbs obliquely up the foreslope to the platform edge between sections 31 to 32. Section 32 is fully platformal in facies. Structural inclinations on the ridge are generally 40 to 60°, providing columnar sections that climb at a high angle to bedding.

The 20-km stretch between sections 12 to 26 (Figure 9) presents a cross-section of a transverse submarine drainage system that was active both before and during the Ghaub glaciation. The drainage system was localized by anomalous subsidence of the Paleoproterozoic crystalline basement. The oldest deposit is glacigenic boulder diamictite (Chuos Formation) limited to a 6 km-wide paleovalley on the basement surface. It is overlain sharply without hiatus by a regionally extensive 'cap' carbonate (Rasthof Formation) comprised of rhythmite, sediment gravity flows and microbialaminite deposited below storm wave base following the Sturtian post-glacial marine transgression. The succeeding "grainstone prism" consists of tabular bedded, intraclastic and oolitic dolostone and subordinate platy dolostone rhythmite. Unlike its correlatives on the platform—the Gruis Formation and Ombaatjie cycles b1-b7 (section 32)—the grainstone prism contains no littoral facies (*e.g.*, tepee microbialaminite) or mappable cycles (parasequences). It is 20 km wide and <600 m thick, and we interpret it to be a complex of submarine channel and levee deposits related to a long-lived foreslope drainage system.

The grainstone prism is succeeded by an extensive blanket of argillite and siltstone (Narachaams Member), locally with density flows carrying outsize quartz granules. The terrigenous incursion is a regional feature associated with the maximum flooding stage of Ombaatjie cycle b8 on the platform (section 32). Notably, it was the only fine-grained terrigenous unit of significance available for erosion during the Ghaub glaciation. It is succeeded by a coarsening-upward stack of dolostone rhythmites and debris flows (Franni-aus Member). The higher debris flows are characterized by very coarse-grained ooids and clasts of ooid grainstone, typically heavily silicified (Figure 10c). The ooids originated in the surf zone but were redeposited after incipient lithification by sediment gravity flows. This facies is not found on the platform and we interpret it as a low-stand wedge associated with falling base-level caused by ice-sheet growth at higher latitudes. A potential correlative of the low-stand wedge is a dolostone aeolianite (cycle b9) locally preserved at the platform edge (Halverson *et al.*, 2002).

Foreslope erosion and sedimentation during the Ghaub glaciation

The glacial marine Ghaub Formation rests on an erosion surface of regional extent (Figure 9). The surface lies

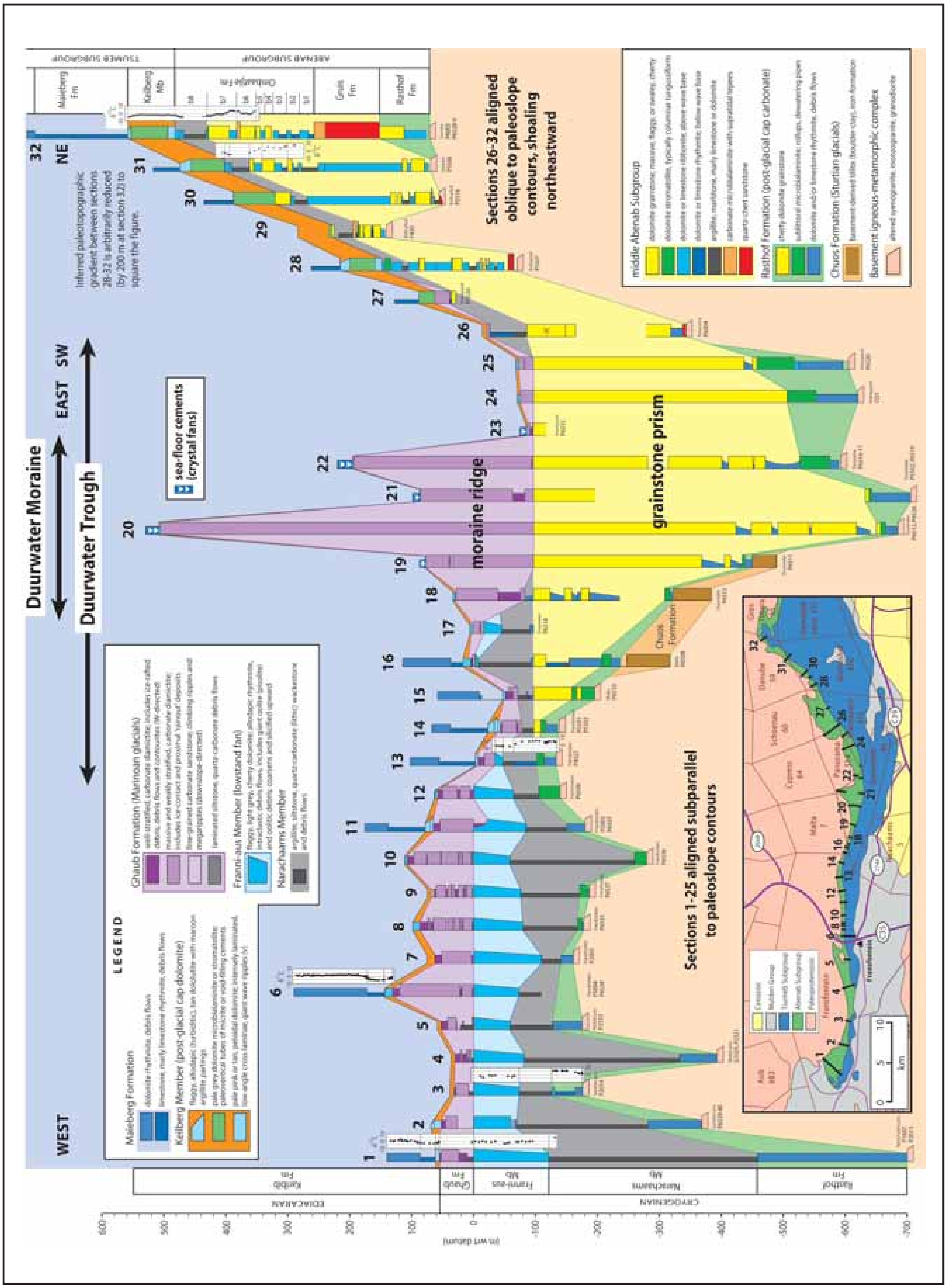

Figure 9. Measured stratigraphic sections (see inset map for locations) of the Abenab and lower Tsumeb Subgroups on the Fransfontein Ridge (Figure 7). See text for interpretation. Datum for sections 1 to 12 is the top of the Franni-aus Member and for sections 14 to 25 is the top of the grainstone prism. Other sections are adjusted to show the interpreted sea-floor topography at the end of the Ghaub glaciation.

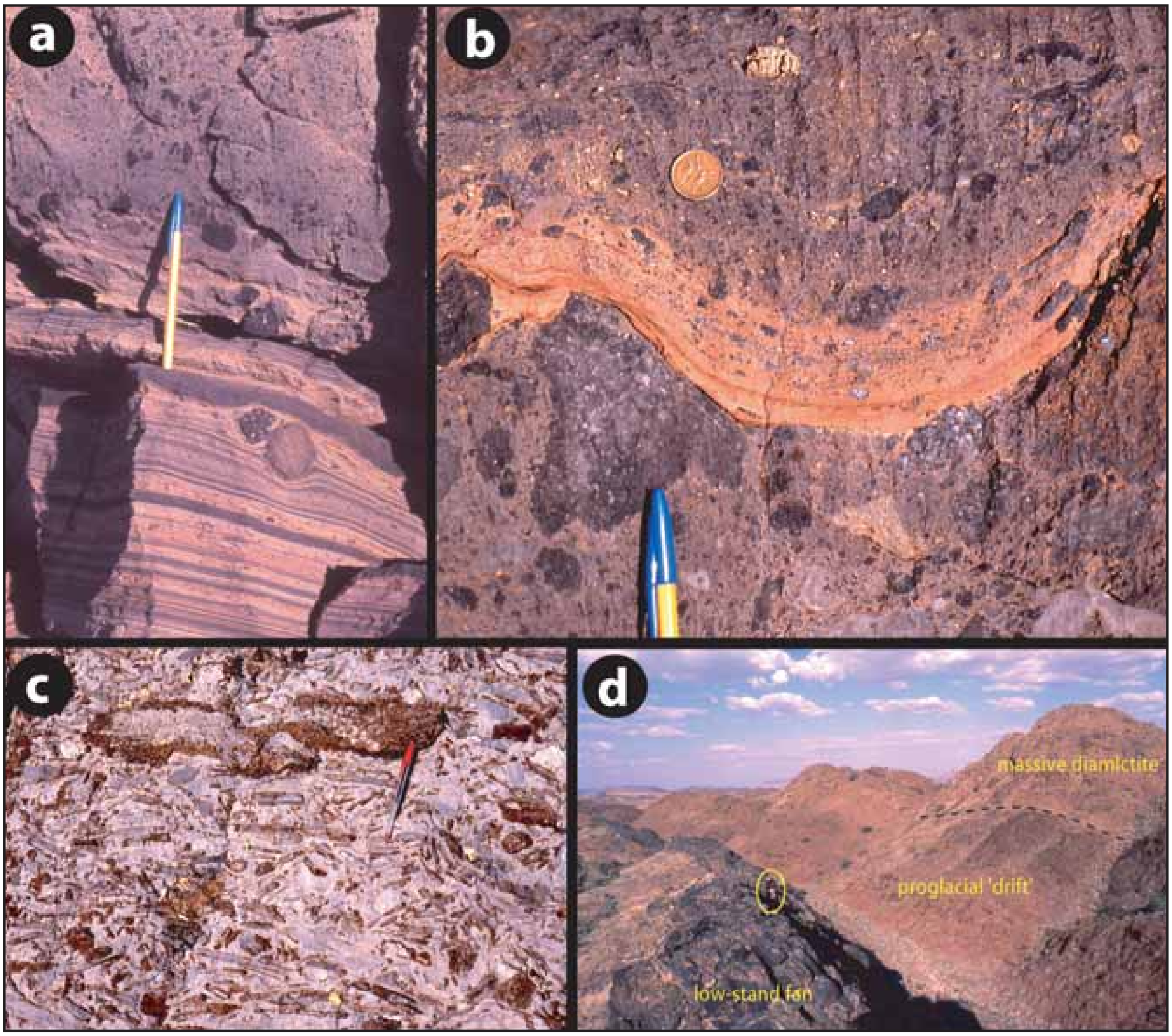

Figure 10. Field photographs from the Fransfontein foreslope (see Figure 9 for locations). (**a**) Stratified proglacial carbonate (grey limestone and tan dolostone) with ice-rafted debris, grading upward into massive 'rain-out' diamictite, Ghaub Formation lower member, section 8. (**b**) Finely laminated 'silt-stringer' within massive diamictite, Ghaub Formation middle member, section 10. The 'silt-stringers' are interpreted to have settled from suspension in meltwater puddles beneath grounded ice. (**c**) Submarine debris flow containing slabs of partially silicified ooid grainstone in the low-stand wedge beneath the Ghaub Formation, Franni-aus Member, section 7. (**d**) Low-stand wedge (Franni-aus Member) overlain by terrigenous siltstone 'drift' of the Ghaub Formation lower member, which grades into massive carbonate diamictite, west end of Bethanis Synclinorium located 58 km southwest of the western terminus of Fransfontein Ridge. The siltstone is the only terrigenous incursion in the Ghaub Formation and is lilkely derived from erosion of the Narachaams Member in the Duurwater Trough (see Figure 9) or equivalent structure.

on the Franni-aus Member west of section 13 and on Ombaatjie cycle b8 east of section 26. Between sections 13 and 26, the surface carves out a broad trough, on the floor of which the Ghaub Formation lies directly upon the grainstone prism. The width of the trough (including a side-valley) is 18 km in the line of section and its axial depth is ~100 m with respect to the undecompacted thickness of eroded footwall strata (*i.e.*, the Narachaams and Franni-aus members on one side and cycle b8 on the other). The trough is centered on farm Duurwater 66 and we call it the *Duurwater Trough* (DT).

The sharply-bounded Ghaub Formation is 40 to 130 m thick west of the DT (Figure 9). Ice advance is recorded by a discontinuous lower member (0 to 14 m thick) composed of stratified proglacial marine sediments with upward-increasing amounts of ice-rafted debris and derived gravity flows (Domack and Hoffman, 2003). In sections 1 to 5, the lower member begins with fine-grained terrigenous sediments (Figure 10d), the only known source for which is the Narachaams Member eroded by the DT (and analogous structures). In sections 11 to 13, the lower member is best preserved in gullies cut in the Franni-aus Member. Terminal ice retreat is recorded by a continuous upper member (3 to 12 m thick) of stratified proglacial carbonates exceptionally rich in ice-rafted debris (Figure 11b). Between the lower and upper members is a complex of vertically and laterally stacked marine 'till tongues' (King *et al.*, 1991; King, 1993)—tongues of unstratified diamictite (Figure 11e) interpreted as ice grounding-line deposits and derived gravity flows. The till tongues are variably limestone-dominated, dolostone-dominated, or of mixed provenance (Figure 12c). The diamictites include true ice-contact deposits as well as proximal 'rain out' from floating ice termini (Domack and Hoffman, 2003). The most common indicator of subglacial deposition are discontinuous 'silt-stringers' (ss, Figure 12c), often delicately laminated and hosting tiny dropstones (Figure 10b). The environment directly seaward of an ice grounding-line is far too turbulent for such fine suspension deposits. Deposition from isolated puddles of meltwater beneath grounded ice is therefore favoured (Domack and Hoffman, 2003). The suspended sediment appears to have originated by 'filter-pressing' of pore water from the subglacial till. The silt-stringers are locally subject to glacio-tectonic folding and thrusting. The till-tongues are separated by m-scale partings of stratified proglacial deposits (Figure 10a, 11d) representing grounding-line retreats and readvances (Condon *et al.*, 2002). These grounding-line oscillations could have been paced by orbital forcing or by stochastic processes (*e.g.*, ice sheet dynamics) on suborbital timescales. Lenses of fine grainstone with southerly-directed climbing ripples (Figure 11c) could be proglacial or subglacial. Stacked recessional till-tongues of comparable thickness and character were deposited in shelf-tranverse troughs on the western Canadian margin during the last (Late Wisconsinian) glacial retreat (Josenhaus, 1997).

The Ghaub Formation thins to <40 m on the walls of the DT, but thickens enormously in the trough axis to 602 and 289 m in sections 20 and 22, respectively (Figure 9). The thickness maxima are separated by an axial depression, 1.5 km wide, where the thickness is 182 m in section 21 (Figure 12a). The two thickest sections consist exclusively of massive to weakly-stratified diamictite, locally conglomeratic (*i.e.*, clast supported). The largest clasts (cycle b7 stromatolite) are >3.0 m in diameter. Stratigraphic variations in clast and matrix petrology are broadly similar to those west of the DT (Figure 12c), scaled for thickness. The buildup is 7.5 km wide at the base (Figure 12a) and 600 m high above the floor of the trough, giving it an aspect ratio of 0.08 (0.6/7.5) in the plane of section. The steepness (10º average slope) of the assumed ridge-like structure favors a slope transverse (*i.e.*, north to south) orientation. We interpret the ridge of diamictite as a slope-transverse medial moraine. We call it the *Duurwater Moraine* (DM) on account of its location in the axial zone of the DT.

Foreslope sedimentation immediately after the Ghaub glaciation

The ice-rafted debris flux ends abruptly at the top of the Ghaub Formation, which is overlain without hiatus by a transgressive cap dolostone (Keilberg Formation) ranging in thickness from 65 m on the upper foreslope (sections 28 to 32) to <1.0 m on the flanks of the DM. Complete description is beyond the scope of this report. Distinctively pale-colored and compositionally pure, it is intensely laminated for the most part with low-angle cross-laminae defined by graded layers (normal or reverse) of micro- to macropeloids. A number of characteristic structures associated with Marinoan cap dolostones globally are represented on the FR. They include megastromatolites with paleovertical tubular structures (Corsetti and Grotzinger, 2005) in sections 27 to 32, giant wave ripples (Allen and Hoffman, 2005) in sections 11 and 14, and void-filling sheets of early diagenetic, fibrous-isopachous cement (Kennedy *et al.*, 2001) sections 1-22. The cap dolostone is thinnest on the flanks of the DM but the coarsest peloids (<3.0 mm diameter) occur there, suggesting that the subnormal thickness results from winnowing.

The cap dolostone was clearly deposited in the ocean mixed layer, and it is gradationally overlain by marly limestone rhythmite (Maieberg Formation) that was deposited below storm wave-base. Concentrations of redox-sensitive elements (*e.g.*, Ba, reactive Fe, Mn) spike at the dolostone-limestone transition, coincident with a large (negative) shift in ?$^{34}S_{CAS}$ (Hurtgen *et al.*, 2002). The same transition occurs up and down the foreslope and across most of the platform. The inferred paleobathymetric relief on the FR is ~800 m, which is much greater than the mixed-layer depth of 200 to 400 m (Allen and Hoffman, 2005). Accordingly, the cap dolostone must be diachronous, tracking the base-level rise up the foreslope and across the platform. As the textural and compositional changes are broadly coincident in all areas, the latter must also be diachronous. We speculate that the ocean was hyperstratified during the deglaciation as a result of surface warming and meltwater production, with a low-density oxic surface layer overlying cold saline anoxic deepwater that evolved beneath an ice cover over millions of years (Bodiselitch *et al.,* 2005). If the glacio-eustatic rise exceeded the mixed-layer depth, meltwater would also collect in an intermediate layer below the mixed layer. In a simple steady-state transgressive model, the vertical stratigraphic sequence represents an inverted depth section of the ocean: the cap dolostone formed in the mixed layer and the marly limestone rhythmite in the underlying thermocline.

Sea-floor cements composed of pseudomorphosed aragonite crystal fans form localized buildups up to 90 m thick at the edge of the platform west of the FR (Soffer, 1998). They occur in marly limestone rhythmite directly above the cap dolostone. On the FR itself, the platform edge (section 32) is devoid of sea-floor cements, but up to 25 m of macroscopic crystal fans crown the DM, most spectacularly in section 22 where they are selectively silicified (Figure 11a). Less profligate cements occur on the flanks of the moraine and none anywhere else

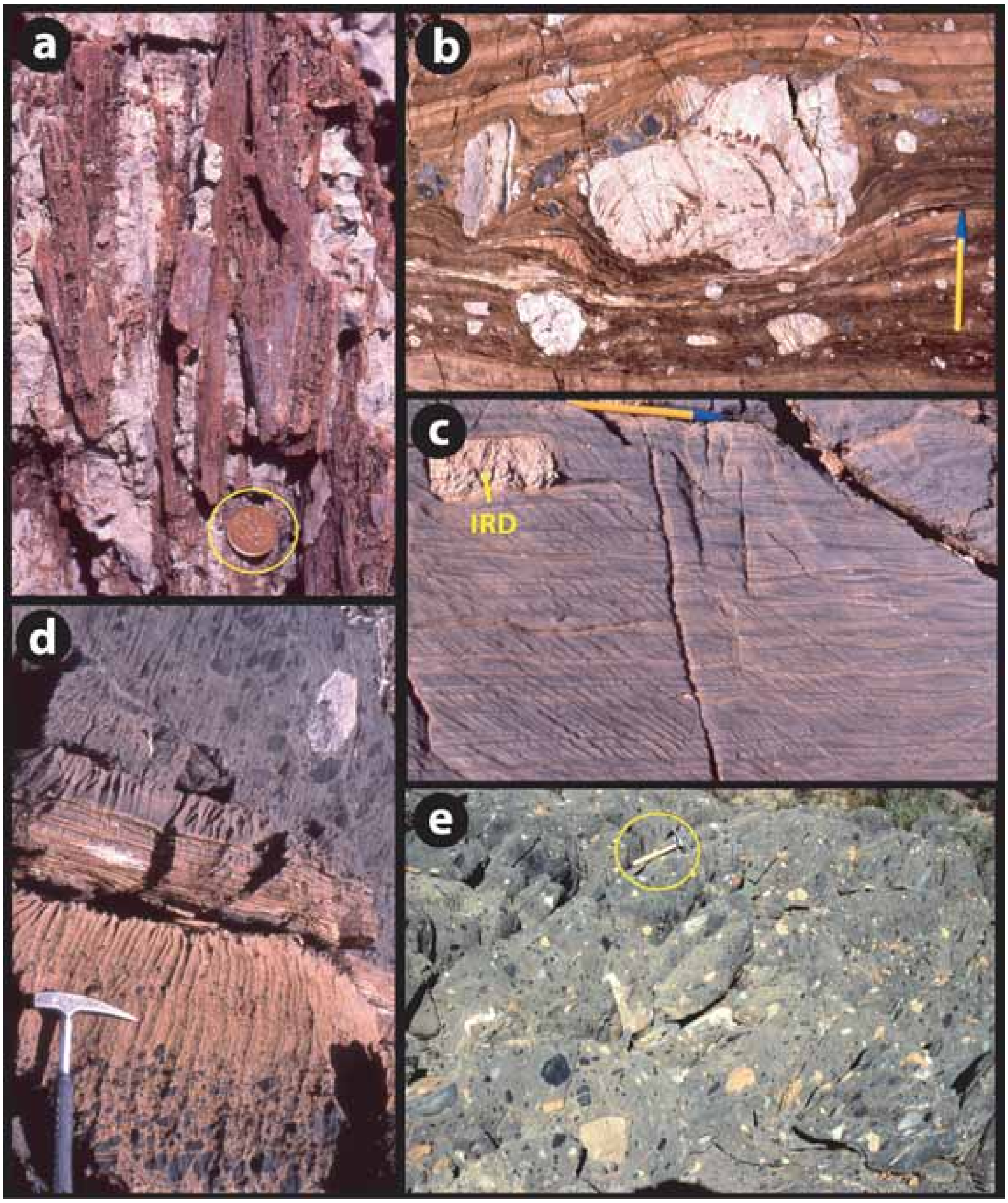

Figure 11. Field photographs from the Fransfontein Ridge (see Figure 9 for locations). (**a**) Silicified sea-floor crystal fans (aragonite pseudomorphs) in the lower Maieberg Formation, directly above the Keilberg cap dolostone on the Duurwater Moraine, section 22. (**b**) Ice-rafted debris (grey limestone and tan dolostone) in stratified proglacial carbonate of the Ghaub Formation upper member, section 12. (**c**) Fine grainstone with southerly-directed climbing ripples seen in oblique section, Ghaub Formation middle member, section 9. Note ice-rafted dropstone in upper left. (**d**) Stratified proglacial carbonate, including climbing ripples produced by contour currents, bounded by limestone-clast diamictites, Ghaub Formation middle member, section 10. Note grading and reverse grading at the top and bottom of the underlying and overlying diamictite, respectively. (**e**) Massive polymictic diamictite with clasts of likmestone (dark grey) and dolostone (tan), Ghaub Formation middle member, section 6.

on the FR. The cements consistently occur in marly limestone rhythmite directly above the (exceptionally thin) cap dolostone, approaching the maximum flooding stage of the post-glacial depositional sequence. Localization of the cements on the moraine may reflect the 'reverse' solubility of calcium carbonate with respect to pressure (*e.g.*, carbonate compensation depth) and/or enhanced ocean mixing associated with sea-floor topography (Garabato *et al.*, 2004).

Discussion

Stokes and Clark (1999) proposed criteria for the recognition of former (*i.e.*, Quaternary) ice streams based on the known characteristics of contemporary ice streams. There are essentially five criteria (Stoker and Bradwell, 2005): (1) characteristic shape and dimensions with convergent flow pattern, (2) rapid flow velocity represented by highly elongate bedforms (*e.g.*, mega-scale lineations), (3) well-delineated margins, (4) deformable bed conditions, and (5) focused sediment delivery in the form of trough-mouth moraine ridges or fans. The Duurwater Trough and Moraine (DTM) cannot meet all these criteria because of the limitations of preservation and exposure (Figure 9). We cannot know the length of the DT but its width (18 km), depth (0.1 km) and shape (broad-floored) are quite similar to

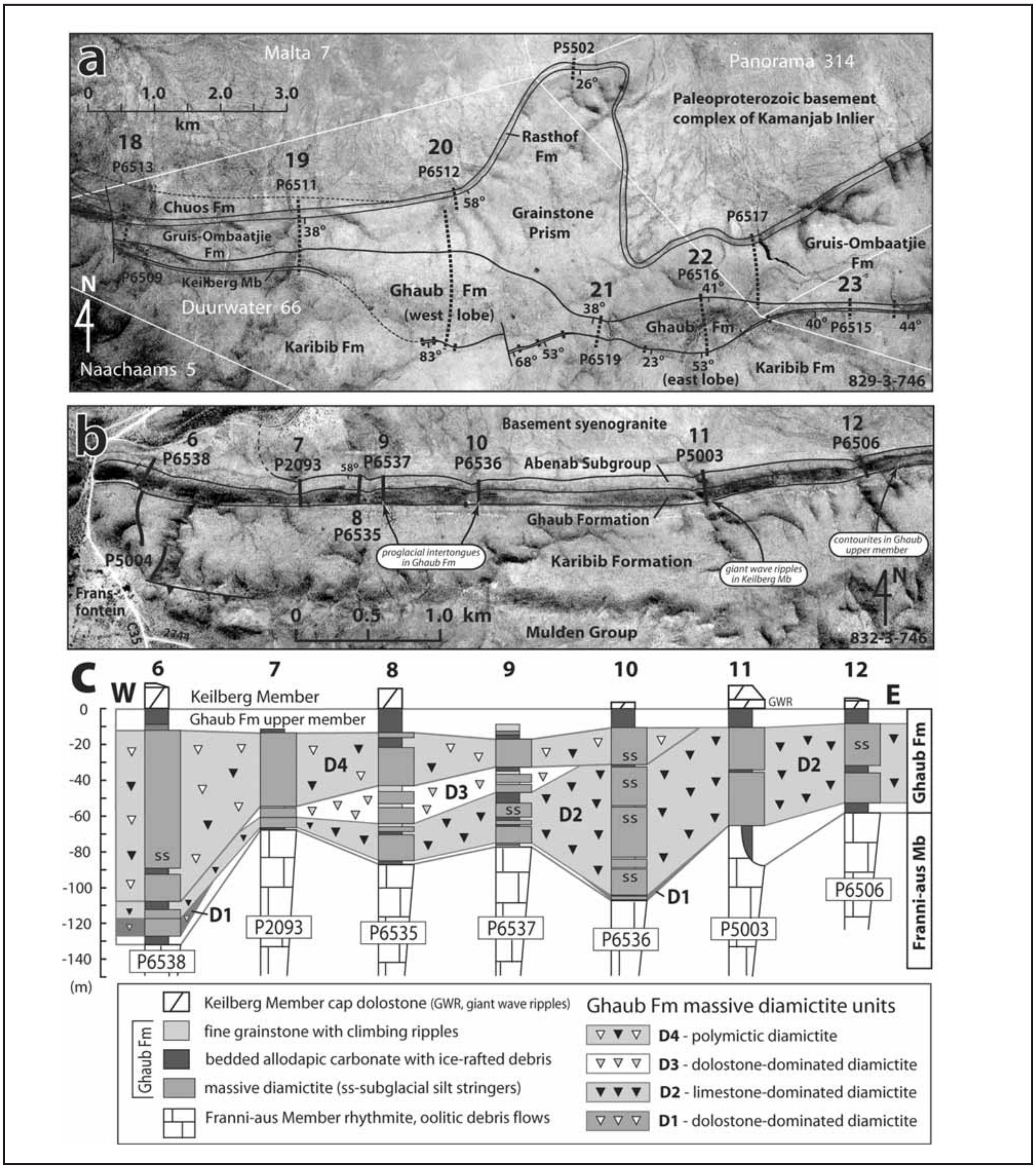

Figure 12. Photomaps and measured columnar sections in key sectors of the Fransfontein Ridge. (**a**) Central sector (sections 18 to 23) showing the double-crested moraine ridge of the Ghaub Formation and the axial zone of the underlying grainstone prism. (**b**) Sector west of the Duurwater Trough (sections 6 to 12) where the internal stratigraphy of the Ghaub Formation is best developed. (**c**) Measured columnar sections of the Ghaub Formation in sections 6-12, showing marine till-tongues separated by thin intervals of stratified proglacial carbonate.

shelf-transverse troughs opposite the major fjords (Isfjorden, Kongfjorden and Bellsund) on the west coast of Svalbard (Ottesen *et al.*, 2005). DT is half the width and twice the depth of the shelf-transverse trough associated with The Minch paleo-ice stream off Scotland (Stoker and Bradwell, 2005), which is dimensionally similar to transverse troughs on the outer shelf off the West Antarctic Peninsula (Heroy and Anderson, 2005). Mega-scale lineations have characteristic amplitudes of 5-10 m and spacing of ~0.3 km (Ó Cofaigh *et al.*, 2002; Ottesen *et al.*, 2005; Heroy and Anderson, 2005): they should in theory be observeable on cross-section on the floor of the DT. In practice, however, this is impossible because the absence of stratigraphic markers in the underlying grainstones, which are unstratified and brecciated. On the other hand, the DT has well-defined lateral margins, evidence of a deformed bed to a depth of ~5 m as is observed beneath a West Antarctic paleo-ice stream (Dowdeswell *et al.*, 2004), and a clear manifestation of focused sediment delivery in the form of the DM. The absence of any proglacial strata in the crestal regions of the DM implies a more stable grounding line or more erosive ice advances, compared with adjacent areas.

The DTM is different from Quaternary ice-stream systems in important ways. Ice stream grounding lines at Quaternary glacial maxima are believed not to have extended beyond the shelf edge on the West Antarctic and Polar North Atlantic margins (Heroy and Anderson, 2005; Ottesen *et al.*, 2005; Stoker and Bradwell, 2005). In contrast, grounding-line wedges including ice-contact diamictite in the Ghaub Formation (Figure 10b) occur 5 to 10 km seaward of the platform edge at an estimated paleodepth on the foreslope of 550 to 800 m. This is however close to the depth range of Quaternary ice-stream grounding zones in the western Ross Sea, Antarctica (Howat and Domack, 2003). The DM has no Quaternary analogs that we know of in terms of its orientation, height and aspect ratio. Sediment buildups near the mouths of Quaternary ice streams have various forms, broadly-conical debris flow fans (Ó Cofaigh *et al.*, 2003; Stoker and Bradwell, 2005), terminal moraine ridges oriented transverse to the ice-stream flowage direction (Ottesen *et al.*, 2005; McMullen *et al.*, in press), and lateral moraine ridges like those on the West Svalbard shelf (Ottesen *et al.*, 2005). Assuming the DM is a ridge in cross-section (600 m is mighty high for a kame), it must be oriented transverse to the slope (on account of its aspect ratio) and therefore parallel to the presumed ice flowage direction. The only way the DM could have been oriented transverse to ice flowage is for the foreslope itself to be the sidewall of a much grander depression occupied by ice flowing westward towards the Adamaster Paleocean (Hartnady *et al.*, 1985). We describe the DM as a medial moraine by virtue of its axial location within the DT, which presupposes a dynamic connection between the ice that cut the DT and that which deposited the DM. This cannot be proved. The existence of a medial moraine is suggestive of a two-pronged tributary system (*e.g.*, The Minch paleo-ice stream). If the two tributaries supplied dominantly limestone and dolostone-chert debris respectively, then the stratigraphic alternations in composition within the DM could relate to changes in discharge ratio between the two tributaries. Lastly, the height (0.6 km) and aspect ratio (0.08) of the DM appear to be larger than any Quaternary moraines associated with ice streams. Possibly this is related to the magnitude and rate of base-level rise that would accompany the meltdown of a global or near-global glaciation (Hyde *et al.*, 2000; Donnadieu *et al.*, 2003; Pollard and Kasting, 2004) or to early lithification of the carbonate debris.

The location of the DTM appears to have been inherited from a long-lived submarine drainage system (the grainstone prism) predating the glaciation. This was ultimately controlled by tectonic subsidence and accommodation as indicated by stratigraphic thickness variations (Figure 9). The easily-eroded argillite and siltstone of the Narachaams Member could account for the depth of the DT but not its location, as they were not exposed until after erosion had breached the more-resistant Franni-aus Member (Figure 9). The tectonic subsidence rate during the Ghaub glaciation, corrected for ice loading, was <0.02 mm per year (recalculated after Halverson *et al.*, 2002) for the platform as a whole. The subsidence rate in the area of the DT 2-3 times greater, based on stratigraphic thickness variations. Accordingly, differential subsidence would have created only ~5 m of relief on the subglacial surface in 10^5 years. A tectonic control on ice sheet dynamics on a flat-topped marine platform is only reasonable if the ice sheet was long-lived like the Antarctic Ice Sheet, which has been in continuous existence since ~14 Ma (Zachos *et al.*, 2001; Holbourn *et al.*, 2005).

Fast-flowing ice streams and paleo-ice streams were wet-base and a deformable sediment layer several meters thick beneath them is arguably critical in accommodating their fast flow (Alley *et al.*, 1986; Dowdeswell *et al.*, 2004). In contrast, slow-moving ice in areas bounding trunk ice streams is cold-base or polythermal, giving rise to surge-type behaviour (Hagen, 1988). Tropical surface temperatures on a snowball Earth would be similar to those on East Antarctica today on account of the high planetary albedo (Donnadieu *et al.*, 2003). The prediction that large tropical ice sheets on a Cryogenian snowball Earth would be drained by fast-moving, wet-base, ice streams (Donnadieu *et al.*, 2003) is supported by our interpretation of the DTM. To the extent that fast-moving, wet-base ice in the Cryogenian is associated with ice streams generally, the argument (McMechan, 2000a; b; Leather *et al.*, 2002; Kellerhals and Matter, 2003) that it is incompatible with a snowball Earth may be groundless.

Terrigenous argillite and siltstone (with minor quartz granules) at the base of the Ghaub Formation in sections 1 to 5 (Figure 9) and farther west (Figure 10d) comprise the only volumetrically significant non-carbonate material deposited during the Ghaub glaciation. Their only logical source is erosion of the lithologically identical Narachaams Member in the DT (and analogous structures). This means, in effect, that the entire Ghaub Formation outside and inside the DT was deposited subsequent to its erosion. If the DT was eroded by an ice stream under glacial maximum conditions, those conditions are not represented by the Ghaub Formation. If other Cryogenian glacial marine sequences are largely or entirely recessional, then evidence they contain may not be diagnostic for glacial maximum conditions as has been assumed (Condon *et al.,* 2002; Corsetti *et al.,* 2003; Allen *et al.,* 2004; Olcott *et al.,* 2005).

Conclusions

The Ghaub Formation on the Fransfontein Ridge consists primarily of marine ice grounding-line diamictites, including ice-contact deposits, which accumulated at paleodepths of 600-800 m on the southern foreslope of the Otavi carbonate platform in northern Namibia. The glacially transported debris is all derived from the then top 60 m of carbonate on the upper foreslope and the platform interior as far as 130 km from the foreslope-platform break. Oscillations of the ice grounding line are recorded by intercalations of stratified proglacial sediments, variably rich in ice-rafted debris, between tongues of diamictite. The time scale of the oscillations (*e.g.,* orbital or stochastic suborbital) is indeterminate with existing data.

The glacial-proglacial succession (60 to 80 m characteristic thickness) rests on a continuous erosion surface that features a broad steep-sided trough, ~100 m deep (relative to underlying stratigraphy) and 18 km wide assuming a slope transverse (north-south) orientation. The Ghaub Formation is 70% thinner inside the trough except in the median zone where a doubly-crested moraine ridge composed of variable but continuous diamictite stands 600 m above the floor of the trough. The ridge is only 7.5 km wide at the base in the line of section and its steepness (aspect ratio of 0.08) implies a slope transverse orientation. Before the glaciation, the area of the trough and moraine ridge was a major submarine drainage system localized by anomalous tectonic subsidence and accommodation. In the post-glacial transgressive sequence, the ‘cap’ dolostone is strongly winnowed and sea-floor cements (former aragonite crystal fans) are preferentially developed on the moraine ridge. This may reflect shoaling and intensified ocean mixing associated with sea-floor topography. The ridge is tentatively interpreted as a medial moraine associated with an ice stream that earlier carved out the trough. The extreme height and steepness of the moraine may reflect the magnitude and rapidity of post-glacial base-level rise, and early cementation of the carbonate debris. The existence of the DTM was “predicted” by the model of Donnadieu *et al.* (2002), wherein tropical Cryogenian ice sheets are drained by fast-moving wet-base ice streams contemporaneous with an ice-covered ocean.

Quartz siltstone at the base of the Ghaub Formation west of the trough is the only volumetrically significant terrigenous incursion. Its probable source is a regionally extensive shale-siltstone unit that was exposed by the erosion of the trough. Accordingly, the entire Ghaub Formation post-dates the erosion of the trough. If the trough was eroded by an ice stream at the glacial maximum (or maxima), then the Ghaub Formation must be entirely recessional in origin. If other Cryogenian glacial successions are recessional, the conditions under which they formed will not be those of the ice maximum.

Epilogue

When Reginald Daly died in 1957, memorials (Billings, 1958; Birch, 1960) were unstinting in their praise of his many and varied contributions—to petrogenesis, the Cordillera, ocean islands, submarine canyons, coral reefs, Lunar origin (a giant impact), and others. Strangely, there was no mention of his steadfast support for continental drift. I doubt this was because his memorialists were opposed to drift: they were of course, but drift was a dead issue by then. I think they simply chose not to drag out what they considered to be an unfortunate lapse of judgment in an otherwise adulatory career. In 1957 the plate tectonics revolution was still 5-10 years off, although the insurrection that bred it was already underway (Irving, 1957). This should serve as a reminder to us all how unexpectedly the wheels of fortune in science can turn.

Acknowledgements

I am grateful to residents and farm owners in northwestern Namibia where I have done field work since soon after independence. John Grotzinger first suggested the area and every encouragement was given me by successive Directors and staff of the Geological Survey of Namibia. Field work for this study was supported by grants from the Earth System History and Geology and Paleontology programmes of the National Science Foundation (USA). Additional support from the Canadian Institute of Advanced Research (Earth System Evolution Program), the Tectonics Special Research Centre (Perth, Australia) and Harvard University is thankfully acknowledged. Enthusiastic field assistance was provided by Cristobal Carman, Hugh Daigle, Jonathon Husson, Gabe Jostrom, and Corey Rennell. Eugene Domack and Michael Hambrey gave important insights on glacial marine sedimentology during visits to Namibia. Gary Clarke, Kurt Grimm and Shawn Marshall made useful suggestions after talks. Galen Halverson and Jonathon Husson carried out the carbon isotopic measurements, and Adam Maloof goaded me to study the glacial record in the first place. The manuscript was critically reviewed by Francis Macdonald and Adam Maloof. Above all I am grateful to the Geological Society of South Africa for the opportunity to honour so great a geologist as Alex. Du Toit.

References

Aitken, J.D. (1991). The Ice Brook Formation and Post-Rapitan, Late Proterozoic glaciation, Mackenzie Mountains, Northwest Territories. *Geological Survey of Canada Bulletin*, **404**, 43pp.

Allen, P.A. and Hoffman, P.F. (2005). Extreme winds and waves in the aftermath of a Neoproterozoic glaciation. *Nature*, **433**, 123-127.

Allen, P., Leather, J. and Brasier, M.D. (2004). The Neoproterozoic Fiq glaciation and its aftermath, Huqf Supergroup of Oman. *Basin Research*, **16**, 507-534, 10.1111/j.1365-2117.2004.00249.x.

Alley, R.B., Blankenship, D.D., Bentley, C.R. and Rooney, S.T. (1986). Deformation of till beneath Ice Stream B, West Antarctica. *Nature*, **322**, 57-59.

Alley, R.B., Blankenship, D.D., Rooney, S.T. and Bentley, C.R. (1989). Sedimentation beneath ice shelves—the view from Ice Stream B. *Marine Geology*, **85**, 101-120.

Bamber, J.L., Vaughan, D.G. and Joughin, I. (2000). Widespread complex flow in the interior of the Antarctic Ice Sheet. *Science*, **287**, 1248-1250.

Baum, S.K. and Crowley, T.J. (2001). GCM response to Late Precambrian (~590 Ma) ice-covered continents. *Geophysical Research Letters*, **28**, 583-586.

Baum, S.K. and Crowley, T.J. (2003). The snow/ice instability as a mechanism for rapid climate change: a Neoproterozoic snowball Earth model example. *Geophysical Research Letters*, **30**, 10.1029/2003GL017333.

Bennett, M.R. (2003). Ice streams as the arteries of an ice sheet: their mechanics, stability and significance. *Earth-Science Reviews*, **61**, 309-339.

Bentley, C.R. (1987). Antarctic ice streams: a review. *Journal of Geophysical Research*, **92**, 8843-8858.

Berger, W. (1982). Increases of carbon dioxide during deglaciation: the coral reef hypothesis. *Naturwissenschaften*, **69**, 87-88.

Billings, M.P. (1958). Reginald A. Daly, Geologist. *Science*, **127**, 19-20.

Birch, F. (1960). Reginald Aldworth Daly. *Biographic Memoirs 1960*, 30-64, National Academy of Sciences (USA), Washington, DC.

Bodiselitsch, B., Koeberl, C., Master, S. and Reimold, W.U. (2005). Estimating duration and intensity of Neoproterozoic snowball glaciations from Ir anomalies. *Science*, **308**. 239-242.

Boetius, A., Ravenschlag, K., Schubert, C.J., Rickert, D., Widdel, F., Giesecke, A., Amman, R., Jørgensen, B.B. and Pfannkuche, O. (2000). A marine microbial consortium apparently mediating anaerobic oxidation of methane. *Nature*, **407**, 623-626.

Brasier, M., McCarron, G., Tucker, R., Leather, J., Allen, P. and Shields, G. (2000). New U-Pb zircon dates for the Neoproterozoic Gubrah glaciation and for the top of the Huqf Supergroup, Oman. *Geology*, **28**, 175-178.

Broecker, W.S. and Peng, T.H. (1982) *Tracers in the Sea*. LDEO Press, Lamont-Doherty Earth Observatory, Palisades, NY.

Brookfield, M.E. (1994). Problems in applying preservation, facies and sequence models to Sinian (Neoproterozoic) glacial sequences in Australia and Asia. *Precambrian Research*, **70**, 113-143.

Budyko, M.I. (1969). The effect of solar radiation variations on the climate of the Earth. *Tellus*, **21**, 611-619.

Canfield, D.E. and Raiswell, R. (1999). The evolution of the sulfur cycle. *American Journal of Science*, **299**, 697-723.

Canfield, D.E. and Teske, A. (1996). Late Proterozoic rise in atmospheric oxygen concentration inferred from phylogenetic and sulfur-isotope studies. *Nature*, **382**, 127-132.

Carey, S.W. and Ahmad, N. (1961). Glacial marine sedimentation. *In:* G. O. Raasch (Editor), Geology of the Arctic, *University of Toronto Press, Toronto, Canada*, 865-894.

Ó Cofaigh, C., Pudsey, C.J., Dowdeswell, J.A. and Morris, P. (2002). Evolution of subglacial bedforms along a paleo-ice stream, Antarctic Peninsula continental shelf. *Geophysical Research Letters*, **29**, 1199, 10.1029/2001GL014488.

Condon, D.J., Prave, A.R. and Benn, D.I. (2002). Neoproterozoic glacial-rainout intervals: observations and implications. *Geology*, **30**, 35-38.

Condon, D., Zhu, M., Bowring, S.A., Wang, W., Yang, A., and Jin, Y. (2005). U-Pb ages from the Neoproterozoic Doushantuo Formation, China. *Science* **308**, 95-98.

Corsetti, F.A. and Grotzinger, J.P. (2005). Origin and significance of tube structures in Neoproterozoic post-glacial cap carbonates: example from Noonday Dolomite, Death Valley, United States. *Palaios*, **20**, 348-363.

Corsetti, F.A., Awramik, S.M., and Pierce, D. (2003). A complex microbiota from snowball Earth times: microfossils from the Neoproterozoic Kingston Peak Formation, Death Valley, USA. *Proceedings of the National Academy of Sciences (USA)*, **100**, 4399-4404.

Crowley, T.J., Hyde, W.T. and Peltier, W.R. (2001). CO_2 levels required for deglaciation of the "Near-Snowball" Earth. *Geophysical Research Letters*, **28,** 283-286.

Daly, R.A. (1947), The Vredefort ring-structure of South Africa. *Journal of Geology*, **55**, 125-145.

De Angelis, H. and Skvarca, P. (2003). Glacier surge after ice shelf collapse. *Science*, **299**, 1560-1562.

Deynoux, M. (1985). Terrestrial or waterlain glacial diamictites? Three case studies from the late Proterozoic and late Ordovician glacial drifts in West Africa. *Palaeogeography, Palaeoclimatology, Palaeoecology*, **51**, 97-141.

Domack, E. and Hoffman, P. (2002). Stratigraphic transition into and out of a snowball glaciation. *Eos, Transactions, American Geophysical Union Fall Meeting*, **84**, 000.

Donnadieu Y., Fluteau, F., Ramstein, G., Ritz, C. and Besse, J. (2003). Is there a conflict between the Neoproterozoic glacial deposits and the snowball Earth interpretation: an improved understanding with numerical modeling. *Earth and Planetary Science Letters*, **208**, 101-112.

Donnadieu, Y., Goddéris, Y., Ramstein, G., Nédélec, A. and Meert, J. (2004a). A 'snowball Earth' climate triggered by continental break-up through changes in runoff. *Nature*, **428**, 303-306.

Donnadieu, Y., Ramstein, G., Goddéris, Y. and Fluteau, F. (2004b). Global tectonic setting and climate of the Late Neoproterozoic: a climate-geochemical coupled study. *In:* G. S. Jenkins, M. A. S. McMenamin, C. P. McKey and L. Sohl, L. (Editors) The Extreme Proterozoic: Geology, Geochemistry, and Climate. *American Geophysical Union, Geophysical Monograph* **146**, 79-89.

Dowdeswell, J.A., Ó Cofaigh, C. and Pudsey, C.J. (2004). Thickness and extent of the subglacial till layer beneath an Antarctic paleo-ice stream. *Geology*, **32**, 13-16.

Du Toit, A.L. (1927). A geological comparison of South America with South Africa. *Carnegie Institution of Washington, Publication*, **381**, 158 pp, 16 plates.

Drewry, D.J. and Copper, A.P.R. (1981). Processes and models of Antarctic glacimarine sedimentation. *Annales of Glaciology*, **2**, 117-122.

Edwards, M.B. (1984). Sedimentology of the Upper Proterozoic glacial record, Vestertana Group, Finnmark, North Norway. *Norges Geologiske Undersøkelse Bulletin*, **394**, 76pp.

Embleton, B.J.J. and Williams, G.E. (1986). Low palaeolatitude of deposition for late Precambrian periglacial varvites in South Australia: implications for paleoclimatology. *Earth and Planetary Science Letters*, **79**, 419-430.

Evans, D.A.D. (2000). Stratigraphic, geochronological, and paleomagnetic constraints upon the Neoproterozoic climatic paradox. *American Journal of Science*, **300**, 347-433.

Eyles, N. (1993). Earth's glacial record and its tectonic setting. *Earth-Science Rev.*, **35**, 1-248.

Eyles, N. and Januszczak, N. (2004). 'Zipper-rift': a tectonic model for Neoproterozoic glaciations during the breakup of Rodinia after 750 Ma. *Earth-Science Reviews*, **65**, 1-73.

Fairchild, I.J. (1993). Balmy shores and icy wastes: the paradox of carbonates associated with glacial deposits in Neoproterozoic times. *In: V.P. Wright, Ed., Sedimentology Review 1*, 1-16, Blackwell Scientific Publications, Oxford.

Fanning, C.M. and Link, P.K. (2004). U-Pb SHRIMP ages of Neoproterozoic (Sturtian) glaciogenic Pocatello Formation, southeastern Idaho. *Geology*, **32**, 881-884, 10.1130/G20609.1.

Gaidos, E.J., Nealson, K.H. and Kirschvink, J.L. (1999). Life in ice-covered oceans. *Science*, **284**, 1631-1633.

Goodman, J. and Pierrehumbert. R.T. (2003). Glacial flow of floating marine ice in "Snowball Earth". *Journal of Geophysical Research*, **108**, 10.1029/2002JC001471.

Gorin, G.E., Racz, L.G. and Walter, M.R. (1982). Late Precambrian-Cambrian sediments of Huqf Group, Sultanate of Oman. *American Association of Petroleum Geologists Bulletin*, **66**, 2609-2627.

Hagen, J.O. (1988). Glacier surge in Svalbard with examples from Usherbreen. *Norsk Geografisk Tidsskrift*, **42**, 203-213.

Halverson, G.P. (in press). A Neoproterozoic chronology. *In:* S. Xiao (Editor), Neoproterozoic Geobiology. *Kluwer Academic Publishers, Delft, Netherlands.*

Halverson, G.P., Hoffman, P.F., Schrag, D.P. and Kaufman, J.A. (2002). A major perturbation of the carbon cycle before the Ghaub glaciation (Neoproterozoic) in Namibia: Prelude to snowball Earth? *Geophysics, Geochemistry, Geosystems*, **3**, 10.1029/2001GC000244.

Halverson, G.P., Hoffman, P.F., Schrag, D.P., Maloof, A.C. and Rice, A.H.N. (2005). Toward a Neoproterozoic composite carbon-isotope record. *Geological Society of America Bulletin*, **117**, 1181-1207, 10.1130/B25630.1.

Hambrey, M.J. and Harland, W.B. (1981). Earth's Pre-Pleistocene Glacial Record. *Cambridge University Press, U.K.*, 1004 pp.

Hambrey, M.J. and Spencer, A.M. (1987). Late Precambrian glaciation of central East Greenland. *Meddelelser om Grønland, Geoscience*, **19**, 50pp.

Harland, W.B. (1964). Evidence of Late Precambrian glaciation and its significance. *In:* A.E.M. Nairn (Editor), Problems in Palaeoclimatology, *Interscience, John Wiley and Sons, London, U.K.*,119-149.

Hartnady, C.J.H., Joubert, P. and Stowe, C.W. (1985). Proterozoic crustal evolution in southwestern Africa. *Episodes*, **8**, 236-244.

Heroy, D.C. and Anderson, J.B. (2005). Ice-sheet extent of the Antarctic Peninsula region during the Last Glacial Maximum (LGM) – Insights from glacial geomorphology. *Geological Society of America Bulletin*, **117**, 1497-1512, 10.1130/B25694.1.

Higgins, J.A. and Schrag, D.P. (2003). Aftermath of a snowball Earth. *Geophysics, Geochemistry, Geosystems*, **4**, 10.1029/2002GC000403.

Hoffman, P.F. (1999). The break-up of Rodinia, birth of Gondwana, true polar wander and the snowball Earth. *Journal of African Earth Sciences*, **28**, 17-33.

Hoffman, P.F. and Halverson, G.P. (in press). Otavi Group of the Northern Platform and the Northern Margin Zone. *In:* R. McG. Miller (Editor), Handbook on the Geology of Namibia. *Geological Survey of Namibia*.

Hoffman, P.F. and Schrag, D.P. (2002). The snowball Earth hypothesis: testing the limits of global change. *Terra Nova*, **14**, 129-155.

Hoffman, P.F., Halverson, G.P. and Schrag, D.P. (2004). On the consistent sequence of mineralogy and bedforms in post-glacial cap carbonates of Marinoan (ca. 635 Ma) age on different paleomargins: steady-state ocean stratification during a post-snowball earth marine transgression? *Geological Society of America, 2004 Annual Meeting Abstracts*. http:gsa.confex.com/gsa/2004AM/finalprogram/abstract_75048.htm

Hoffman, P.F., Kaufman, A.J., Halverson, G.P. and Schrag, D.P. (1998). A Neoproterozoic snowball Earth. *Science*, **281**, 1342-1346.

Hoffmann, K.-H. and Prave, A.R. (1996). A preliminary note on a revised subdivision and regional correlation of the Otavi Group based on glaciogenic diamictites and associated cap dolomites. *Communications of the Geological Survey of Namibia*, **11**, 77-82.

Hoffmann, K.-H., Condon, D.J., Bowring, S.A. and Crowley, J.L. (2004). U-Pb zircon date from the Neoproterozoic Ghaub Formation, Namibia: constraints on Marinoan glaciation. *Geology* **32**, 817-820, 10.1130/G20519.l.

Holbourn, A., Kuhnt, W., Schulz, M. and Erlankeuser, H. (2005). Impacts of orbital forcing and atmospheric carbon dioxide on Miocene ice-sheet expansion. *Nature*, **438**, 483-487.

Howat, J.M. and Domack, E.W. (2003). Reconstructions of western Ross Sea palaeo-ice-stream grounding zones from high-resolution acoustic stratigraphy. *Boreas*, **32**, 56-75.

Hurtgen, M.T., Arthur, M.A. and Halverson, G.P. (2002). Constraining perturbations to the sulfur cycle in the aftermath of snowball earth: geochemistry of the Neoproterozoic Maieberg Formation, Namibia. *Geological Society of America, 2002 Annual Meeting Abstracts*. http://gsa.confex.com/gsa/2002AM/finalprogram/abstract_45548.htm

Hyde, W.T., Crowley, T.J., Baum, S.K. and Peltier, W.R. (2000). Neoproterozoic 'snowball Earth' simulations with a coupled climate/ice-sheet model. *Nature*, **405**, 425-429.

James, N.P., Narbonne, G.M. and Kyser, T.K. (2001). Late Neoproterozoic cap carbonates: Mackenzie Mountains, northwestern Canada: precipitation and global glacial meltdown. *Canadian Journal of Earth Sciences*, **38**, 1229-1262.

Jenkins, G.S. and Smith, S.R. (1999). GCM simulations of Snowball Earth conditions during the late Proterozoic. *Geophysical Research Letters*, **26**, 2263-2266.

Jiang, G., Kennedy, M.J., and Christie-Blick, N. (2003). Stable isotopic evidence for methane seeps in Neoproterozoic postglacial cap carbonates. *Nature* **426**, 822-826.

Kappler, A., Pasquero, C., Konhauser, K.O. and Newman, D.K. (2005). Deposition of banded iron formations by anoxygenic phototrophic Fe(II)-oxidizing bacteria. *Geology*, **33**, 865-868, 10.1130/G21658.1

Kasemann, S.A., Hawkesworth, C.J., Prave, A.R., Fallick, A.E. and Pearson, P.N. (2005). Boron and calcium isotope composition in Neoproterozoic carbonate rocks from Namibia: evidence for extreme environmental change. *Earth and Planetary Science Letters*, **231**, 73-86.

Kaufman, A.J., Knoll, A.H. and Narbonne, G.M. (1997). Isotopes, ice ages, and terminal Proterozoic earth history. *Proceedings of the National Academy of Sciences (USA)*, **94**, 6600-6605.

Kellerhals, P. and Matter, A. (2003). Facies analysis of a glaciomarine sequence, the Neoproterozoic Mirbat Sandstone Formation, Sultinate of Oman. *Eclogae Geologicae Helviticae*, **96**, 49-70.

Kempf, O., Kellerhals, P., Lowrie, W. and Matter, A. (2000). Paleomagnetic directions in Late Precambrian glaciomarine sediments of the Mirbat Sandstone Formation, Oman. *Earth and Planetary Science Letters*, **175**, 181-190.

Kennedy, M.J. (1996). Stratigraphy, sedimentology, and isotope geochemistry of Australian Neoproterozoic postglacial cap dolostones: deglaciation, $d^{13}C$ excursions, and carbonate precipitation. *Journal of Sedimentary Research*, **66**, 1050-1064.

Kennedy, M.J., Christie-Blick, N. and Sohl, L.E. (2001). Are Proterozoic cap carbonates and isotopic excursions a record of gas hydrate destabilization following Earth's coldest intervals. *Geology*, **29**, 443-446.

Kennedy, M.J., Runnegar, B., Prave, A.R., Hoffmann, K.-H. and Arthur, M.A. (1998). Two or four Neoproterozoic glaciations? *Geology*, **26**, 1059-1063.

Kilner, B., Mac Niocaill, C. and Brasier, M. (2005). Low-latitude glaciation in the Neoproterozoic of Oman. *Geology*, **33**, 413-416.

King, L.H. (1993) Till in the marine environment. *Journal of Quaternary Science*, **8**, 347-358.

King, L.H., Rokoengen, K., Fader, G.B.J., and Gunleiksrud, T. (1991). Till-tongue stratigraphy. *Geological Society of America Bulletin*, **103**, 637-659.

Kirschvink, J.L. (1992). Late Proterozoic low-latitude glaciation: the snowball Earth. *In: Schopf, J.W. and Klein, C., Eds., The Proterozoic Biosphere*, Princeton Univ. Press, New York, 51-52.

Klein, C. and Beukes, N.J. (1993). Sedimentology and geochemistry of the glaciogenic late Proterozoic Rapitan iron-formation in Canada. *Economic Geology*, **84**, 1733-1774.

Klein, C. and Ladeira, E.A. (2004). Geochemistry and mineralogy of Neoproterozoic banded iron-formations and some selected, siliceous manganese formations from the Urucum District, Mato Grosso do Sul, Brazil. *Economic Geology*, **99**, 1233-1244.

Knoll, A.H., Hayes, J.M., Kaufman, A.J., Swett, K. and Lambert, I.B. (1986). Secular variation in carbon isotope ratios from Upper Proterozoic successions of Svalbard and East Greenland. *Nature* **321**, 831-838.

Knoll, A.H., Walter, M.R., Narbonne, G.M. and Christie-Blick, N. (2004). A new Period for the geologic time scale. *Science*, **305**, 621-622.

Kump, L.R. and Seyfried, W.E., Jr. (2005). Hydrothermal Fe fluxes during the Precambrian: effect of low oceanic sulfate concentrations and low hydrostatic pressure on the composition of black smokers. *Earth and Planetary Science Letters*, **235**, 654-662.

Leather, J., Allen, P.A., Brasier, M.D. and Cozzi, A. (2002). Neoproterozoic snowball Earth under scrutiny: evidence from the Fiq glaciation of Oman. *Geology*, **30**, 891-894.

Lewis, J.P., Weaver, A.J., Johnston, S.T., and Eby, M. (2003). Neoproterozoic "snowball Earth": Dynamic sea ice over a quiescent ocean. *Paleoceanography*, **18**, 10.1029/2003PA000296.

Lindzen, R.S. and Farrell, B. (1977). Some realistic modifications of simple climate models. *Journal of Atmospheric Sciences*, **34**, 1487-1500.

MacGabhann, B.A. (2005). Age constraints on Precambrian glaciations and the subdivision of Neoproterozoic time. IGCP Project 512 Report, 13 p.

Macouin, M., Besse, J., Ader, M., Gilder, S., Yang, Z., Sun, Z. and Agrinier, P. (2004). Combined paleomagnetic and isotopic data from the Doushantuo carbonates, South China: implications for the "snowball Earth" hypothesis. *Earth and Planetary Science Letters*, **224**, 387-398.

Maloof, A.C., Halverson, G.P., Kirschvink, J.L., Schrag, D.P., Weiss, B.P., and Hoffman, P.F. (in press). Combined paleomagnetic, isotopic and stratigraphic evidence for true polar wander from the Neoproterozoic Akademikerbreen Group, Svalbard. *Geological Society of America Bulletin*.

Marshall, H.G., Walker, J.C.G. and Kuhn, W.R. (1988). Long-term climate change and the geochemical cycle of carbon. *Journal of Geophysical Research*, **93**, 791-801.

Martin, H. (1965). *Beobachtungen zum Problem der jung-präkambrischen Glazialen Ablagerungen in Südwestafrika* (Observations concerning the problem of the late Precambrian glacial deposits in South West Africa). *Geologische Rundschau*, **54**, 115-127.

McKay, C.P. (2000). Thickness of tropical ice and photosynthesis on a snowball Earth. *Geophysical Research Letters*, **27**, 2153-2156.

McMechan, M.E. (2000a). Vreeland Diamictites—Neoproterozoic glaciogenic slope deposits, Rocky Mountains, northeast British Columbia. *Bulletin of Canadian Petroleum Geology*, **48**, 246-261.

McMechan, M.E. (2000b). Reply to discussion: Vreeland Diamictites – Neoproterozoic glaciogenic slope deposits, Rocky Mountains, northeast British Columbia. *Bulletin of Canadian Petroleum Geology*, **48**, 364-366.

McMullen, K., Domack, E., Leventer, A., Olson, C., Dunbar, R. and Brachfeld, S. (in press). Glacial morphology and sediment formation in the Mertz Trough, East Antarctica. *Palaeogeography, Palaeoclimatology, Palaeoecology*.

Meert, J.G. and Torsvik, T.H. (2004). Paleomagnetic constraints on Neoproterozoic 'Snowball Earth' continental reconstructions. *In:* G. S. Jenkins, M. A. S. McMenamin, C. P. McKey, C.P. and L. Sohl (Editors), The Extreme Proterozoic: Geology, Geochemistry, and Climate. *American Geophysical Union Geophysical Monograph*, **146**, 5-11.

Moreau, J., Ghienne, J.F., Le Heron, D.P., Rubino, J.L. and Deynoux, M. (2005). 440 Ma ice stream in North Africa. *Geology*, **33**, 753-756, 10.1130/G21782.1.

Narbonne, G.M. and Aitken, J.D. (1995). Neoproterozoic of the Mackenzie Mountains, northwestern Canada. *Precambrian Research*, **73**, 101-121.

Naveira Garabato, A.C., Polzin, K.L., King, B.A., Heywood, K.J. and Visbeck, M. (2004) Widespread intense turbulent mixing in the Southern Ocean. *Science*, **303**, 210-213.

Nogueira, A.C.R., Riccomini, C., Sial, A.N., Moura, C.A.V. and Fairchild, T.R. (2003). Soft-sediment deformation at the base of the Neoproterozoic Puga cap carbonate (southwestern Amazon craton, Brazil): confirmation of rapid icehouse to greenhouse transition in snowball Earth. *Geology*, **31**, 613-616.

North, G.R., Cahalan, R.F. and Coakley, J.A.Jr. (1981). Energy balance climate models. *Reviews of Geophysics and Space Physics*, **19**, 91-121.

Olcott, A.N., Sessions, A.L., Corsetti, F.A., Kaufman, A.J. and de Oliveira, T.F. (2005). Biomarker evidence for photosynthesis during Neoproterozoic glaciation. *Science*, **310**, 471-474.

Orheim, O. and Elverhøi, A. (1981). Model for submarine glacial deposition. *Annales of Glaciology*, **2**, 123-128.

Ottesen, D., Dowdeswell, J.A. and Rise, L. (2005). Submarine landforms and the reconstruction of fast-flowing ice streams within a large Quaternary ice sheet: The 2500-km-long Norwegian—Svalbard margin (57º–80ºN). *Geological Society of America Bulletin*, **117**, 1033-1050, 10.1130/B25577.1.

Park, J.K. (1997). Paleomagnetic evidence for low-latitude glaciation during deposition of the Neoproterozoic Rapitan Group, Mackenzie Mountains, N.W.T., Canada. *Canadian Journal of Earth Sciences*, **34**, 34-49.

Peltier, W.R., Tarasov, L., Vettoretti, G. and Solheim, L.P. (2004). Climate dynamics in deep time: modeling the "snowball bifurcation" and assessing the plausibility of its occurrence. *In:* G. S. Jenkins, M. A. S. McMenamin, C. P. McKey and L. Sohl (Editors), The Extreme Proterozoic: Geology, Geochemistry, and Climate. *American Geophysical Union, Geophysical Monograph*, **146**, 107-124.

Pierrehumbert, R.T. (2004). High levels of atmospheric carbon dioxide necessary for the termination of global glaciation. *Nature*, **429**, 646-649.

Pierrehumbert, R.T. (2005). Climate dynamics of a hard snowball Earth. *Journal of Geophysical Research*, **110**, D01111, 10.1029/2004JD005162.

Plumb, K.A. (1991). New Precambrian time scale. *Episodes*, **14**, 139-140.

Pollard, D. and Kasting, J.F. (2004). Climate-ice sheet simulations of Neoproterozoic glaciation before and after collapse to Snowball Earth. *In:* G. S. Jenkins, M. A. S. McMenamin, C. P. McKey and L. Sohl (Editors), The Extreme Proterozoic: Geology, Geochemistry, and Climate. *American Geophysical Union*, *Geophysical Monograph*, **146**, 91-105.

Pollard, D. and Kasting, J.F. (2005). Snowball Earth: a thin-ice solution with flowing glaciers. *Journal of Geophysical Research*, **110**, C07010, 10.1029/2004JC002525.

Preiss, W.V. (1987). The Adelaide Geosyncline: Late Proterozoic stratigraphy, sedimentation, palaeontology and tectonics. *Geological Survey of South Australia Bulletin*, **53**, 438pp.

Ridgwell, A. and Kennedy, M. (2004). Secular changes in the importance of neritic carbonate deposition as a control on the magnitude and stability of Neoproterozoic ice ages. *In:* G. S. Jenkins, M. A. S. McMenamin, C. P. McKey and L. Sohl (Editors), The Extreme Proterozoic: Geology, Geochemistry, and Climate. *American Geophysical Union, Geophysical Monograph*, **146**, 55-72.

Ridgwell, A.J., Kennedy, M. and M.J. Caldeira, K. (2003). Carbonate deposition, climate stability, and Neoproterozoic ice ages. *Science*, **302**, 859-862.

Roberts, J.D. (1976). Late Precambrian dolomites, Vendian glaciation, and synchroneity of Vendian glaciations. *Journal of Geology*, **84**, 47-63.

Schmidt, P.W. and Williams, G.E. (1995). The Neoproterozoic climatic paradox: equatorial paleolatitude for Marinoan glaciation near sea level in South Australia. *Earth and Planetary Science Letters*, **134**, 107-124.

Schmidt, P.W., Williams, G.E. and Embleton, B.J.J. (1991). Low palaeolatitude of Late Proterozoic glaciation: early timing of remnance in Haematite of the Elatina Formation, South Australia. *Earth and Planetary Science Letters*, **105**, 355-367.

Schrag, D.P., Berner, R.A., Hoffman, P.F. and Halverson, G.P. (2002). On the initiation of a snowball Earth. *Geophysics, Geochemistry, Geosystems*, **3**, 10.1029/2001GC000219.

Sellers, W.D. (1969). A global climatic model based on the energy balance of the Earth-atmosphere system. *Journal of Applied Meteorology*, **8**, 392-400.

Shields, G.A. (2005). Neoproterozoic cap carbonates: a critical appraisal of existing models and the plumeworld hypothesis. *Terra Nova*, **17**, 299-310.

Soffer, G. (1998). Evolution of a Neoproterozoic continental margin subject to tropical glaciation. *Unpublished B.A. Thesis, Harvard College, Cambridge, Massachusetts, USA*, **Please provide number of pages**.

Sohl, L.E., Christie-Blick, N. and Kent, D.V. (1999). Paleomagnetic polarity reversals in Marinoan (ca. 600 Ma) glacial deposits of Australia: implications for the duration of low-latitude glaciations in Neoproterozoic time. *Geological Society of America Bulletin*, **111**, 1120-1139.

Spencer, A.M. (1971). Late Pre-Cambrian glaciation in Scotland. *Memoirs of the Geological Society of London*, **6**, 98pp, 11 plates.

Stoker, M. and Bradwell, T. (2005). The Minch palaeo-ice stream, northwest sector of the British—Irish Ice Sheet. *Journal of the Geological Society*, **163**, 425-428.

Stokes, C.R. and Clark, C.D. (1999). Geomorphological criteria for identifying Pleistocene ice streams. *Annals of Glaciology*, **28**, 67-74.

Thomas, D.N. and Dieckmann, G.S. (2002). Antarctic sea ice—a habitat for extremophiles. *Science*, **295**, 641-644.

Trindade, R.I.F., Font, E., D'Agrella-Filho, Nogueira, A.C.R. and Riccomini, C. (2003). Low-latitude and multiple geomagnetic reversals in the Neoproterozoic Puga cap carbonate, Amazon craton. *Terra Nova*, **15**, 441-446, 10.1046/j.1365-3121.2003.00510.x.

Walter, M.R., Veevers, J.J., Calver, C.R., Gorjan, P. and Hill, A.C. (2000). Dating the 840-544 Ma Neoproterozoic interval by isotopes of strontium, carbon, and sulfur in seawater, and some interpretive models. *Precambrian Research*, **100**, 371-433.

Walker, J.C.G., Hays, P.B. and Kasting, J.F. (1981). A negative feedback mechanism for the long-term stabilization of Earth's surface temperature. *Journal of Geophysical Research*, **86**, 9776-9782.

Warren, S.G., Brandt, R.E., Grenfell, T.C. and McKay, C.P. (2002). Snowball Earth: ice thickness on the tropical ocean. *Journal of Geophysical Research*, **107** (C10), 10.1029/2001JC001123.

Whitten, G.F. (1970). The investigation and exploration of the Razorback Ridge iron deposit. *Geological Survey of South Australia, Report of Investigations*, **33**, 151pp.

Williams, G.E. (1979). Sedimentology, stable-isotope geochemistry and palaeoenvironment of dolostones capping late Precambrian glacial sequences in Australia. *Journal of the Geological Society of Australia*, **26**, 377-386.

Worseley, T.R. and Kidder, D.L. (1991). First-order coupling of paleogeography and CO_2, with global surface temperature and its latitudinal contrast. *Geology*, **19**, 1161-1164.

Zachos, J., Pagani, M., Sloan, L., Thomas, E. and Billups, K. (2001).Trends, rhythms, and aberrations in global climate 65 Ma to Present. *Science*, **292**, 686-693.

Editorial handling: J. M. Barton Jr.